NTNU

Norwegian University of
Science and Technology

Evaluation of Chilled Methanol Processes for Acid Gas Removal

Manuel Piña Dreyer

Natural Gas Technology
Submission date: June 2011
Supervisor: Arne Olav Fredheim, EPT

Norwegian University of Science and Technology
Department of Energy and Process Engineering

PREFACE

The current master thesis is the outcome of six months of joint work between the Institute of Energy and Processing of the Norwegian University of Science and Technology (NTNU) and the Statoil Research and Development (R&D) Center in Trondheim, Norway.

This thesis counts as the degree project of the five years Chemical Engineering Diploma of Universidad Simón Bolívar in Caracas, Venezuela. It was developed during the second semester of the academic exchange year 2010-2011.

The project was sketched and supervised by Professor Arne Olav Fredheim from the previously mentioned department; who also works in the Statoil R&D Center. Dr. Even Solbraa and Dr. Eivind Johannessen were also responsible for the supervision and direction of the project, both working in the Research and Development Center of Statoil in Trondheim. Also, Professor Freddy Figueira from the Department of Thermodynamics and Transport Phenomena oversaw the project from Universidad Simon Bolívar.

The aim of the thesis is to present a complete study about the low temperature absorption of acid gas contaminants present in natural gas with physical solvents such as methanol.

Manuel Alejandro Piña Dreyer

Norwegian University of Science and Technology (NTNU)

Trondheim, Norway

June, 2011

ACKNOWLEDGMENTS

First of all, I would like to thank my tutors, both here and in Venezuela. Without them the project would have not existed in first place and could not have been completed. Professors Arne Olav Fredheim and Freddy Figueira; Drs. Even Solbraa and Eivind Johannessen, thank you all very much.

Furthermore, I would like to thank both the Institute of Energy and Processing of NTNU and the Statoil Research and Development Center for letting me be part of your team for these six months.

Thanks also to my coordinators in Venezuela, Elena Úrsula Ehrmann and Daniel González for advising and helping me along all the process of thesis and the exchange year. Your presence has been very important, indeed. Thanks to NTNU and Universidad Simón Bolívar for letting students like me to be part of such amazing experiences like this exchange year. Also, thanks to my teacher Sabrina Di Scipio; who has always been an excellent mentor along my studies.

My gratitude is also extended to my family and friends in Venezuela, to whom I love and appreciate deeply. Furthermore, thanks to my new family here in Norway: my exchange year friends. You have understood and felt my worries and happiness regarding this project along with me; this being priceless. I will always cherish and value our friendship.

Special thanks to Facund Fortuny, a.k.a as “Fei”. You became my brother during this year and I will not have completed this project without you being after me, waking me up every morning to work more.

Thanks to all who believed in me and helped me to be where I am now.

ABSTRACT

As the main goal achieved with this master thesis, a plant design was modeled for an acid gas removal process with methanol operating at low temperatures. First, a bibliographical research was made in terms of sour gas treatment; with special focus of physical absorption processes involving methanol as the solvent to achieve separation; such as *Rectisol* and *Ifpexsol*. The literature research was extended to thermodynamic data; compiling equilibrium values for binary systems between methanol and carbon dioxide (CO_2), hydrogen sulphide (H_2S) and methane (CH_4); respectively.

The simulator Pro II with Provision was selected as the computational tool to achieve thermodynamic calculations for the gas stream to be treated. The thermodynamic Equation of State (EOS) utilized to model the properties of the system was a simulator built in modified version of the Soave-Redlich-Kwong-Panagiotopuolos-Reid EOS.

Comparisons between the researched equilibrium values and the simulated data were done; corroborating that the model was strong enough to perform calculations for components related with acid gas removal.

A natural gas stream rich in Carbon Dioxide (CO_2), Nitrogen (N_2) and heavy-hydrocarbons was selected from Statoil's Snøhvit gas treatment processing in order to be subject of acid gas removal. The plant design for the sour gas treatment was developed in three individual stages that were later integrated: heavy-hydrocarbons removal, absorption with methanol and solvent regeneration. The design proposed was effective into removing the CO_2 present in the natural gas stream down to a value of 40 ppmv.

Finally, a brief *pinch analysis* was sketched; thus identifying the actual possibility of heat integrating the system with an LNG processing unit. In conclusion, simple simulation and thermodynamic tools can conduct to efficient designs for integral acid gas removal plants.

TABLE OF CONTENTS

LIST OF ABBREVIATIONS

atm	Pressure in atmospheres
bara	Absolute pressure in bar
bscm	Billion standard cubic meters
C1	Methane
C2	Ethane
C3	Propane
C5	Pentanes
CCS	Carbon Capture and Storage
CH_4	Methane
CO_2	Carbon Dioxide
CX+	Hydrocarbons over X C-atoms
DEA	Diethanolamine
EOS	Equation of State
H_2S	Hydrogen Sulphide
HHC	Heavy Hydrocarbon
i-C4	Isobutane
IFPEX-1	First Steps of the *Ifpexol* process
IFPEX-2	Final Steps of the *Ifpexol* process

K_2CO_3	Potassium Carbonate
Kg-mole/h	Kilogram-mole per hour
LNG	Liquified Natural Gas
MEA	Monoethanolamine
MeOH	Methanol
MSm^3/day	Million standard cubic meters per day
N_2	Nitrogen
n-C4	n-Butane
NGL	Gas Condensates
NH_3	Ammonia
PFD	Process Flow Diagram
ppmv	Parts per million in a volumetric basis
PVT	Pressure, Volume and Temperature conditions
R/P	Resources-to-production ratio
SRK	Soave-Redlich-Kwong Equation of State
W	Work

LIST OF TABLES

LIST OF FIGURES

1. INTRODUCTION

When giving a quick glimpse to human history, sufficient information sustains that the development of society is closely tied with the increase of energy demand. Events like wars, science breakthroughs and even the current globalization phenomenon could not be happening without a strong energy sector behind them. During the last 50 years, half of the energy ever produced by man was consumed [1]; the same period when humankind arrived to the moon, developed the internet, decoded the human genome, etc.

Energy demand is expected to continue increasing, especially due to the rapid growth of giant societies like China, India and Brazil. Nevertheless, the consumption of energy comes affiliated with environmental consequences; this challenges the panorama of a sustainable future for the planet.

As can be seen in Figure 1.1, the main source of energy nowadays comes from the fossil fuel sector, thus representing more than 80 % of the total energy produced. Among these, natural gas covers alone around 23% of the production, positioning itself as the third source of energy [1]. Nevertheless, these fossil fuels compose the main production source of greenhouse gases, thus contributing with the current global climate change [2].

According the U.S. Energy Information Agency, the natural gas industry is expected to grow 44% until 2035. Several countries are taking measurements to shift from the dominating oil and coal industries towards natural gas in order to become “greener”; since this is the fossil fuel that produces less greenhouse emissions. This tendency is becoming clearer for newly developed plants, where the electric power supply is preferred to be generated from natural gas fuel turbines [3].

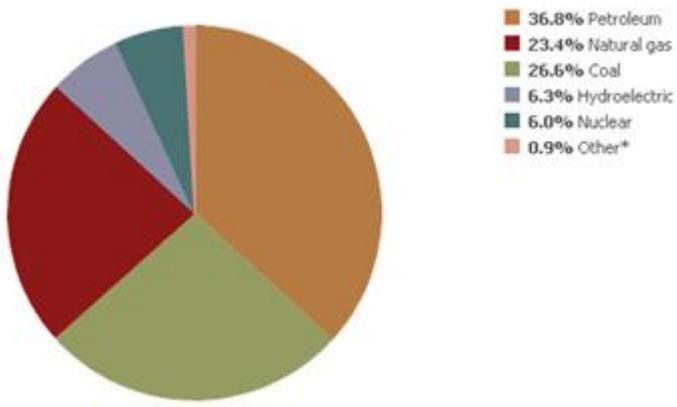

Figure 1.1. Energy world production chart by sectors-2009 [1]

Also, at the current production rate with the current resources available (reserves-to-production ratio, R/P) [4], natural gas persists in the future longer than oil; with an R/P of 60 years vs. 43 years for oil [1].

Hence, the importance of the industry becomes evident in order to supply the energy demand in the future. The development of its resources is, therefore, a main subject of discussion within the energy sector. From these resources, almost 30 % had to be subject of sour gas treatment due to high concentrations of acidic substances (CO_2 and H_2S) [5].

To be able to efficiently produce the totality of the resources remaining, acid gas treatment will have to be considered as an important strategy of the future natural gas processing.

Several strategies exist to remove these acid contaminants from the natural gas stream; among these the physical absorption. Methanol is one of the solvents used, being efficient to remove these contaminants due to high solubility values at low temperatures [6]. This coupled with its vast market availability, makes out of

Methanol based processes an attractive alternative to design acid gas removal facilities.

The aim of this master thesis is to study and design a simple chilled (low temperature) methanol based process; while presenting alternatives to make out of this operation an optimal and efficient one. First, a conceptual base is formulated from fundamental notions about acid gas removal and thermodynamic modeling. Then, simulations are conducted in order to obtain a plant design for an acid gas removal process within a natural gas treatment line. Finally, a brief addressing of the feasibility of heat integrating the acid gas removal unit design with an LNG processing facility is presented.

2. ACID GAS REMOVAL

During the current section of the text, definitions regarding acid gas (also known as sour gas) treatment are to be discussed. Once basic concepts are presented, information about absorption processes as a way to achieve acid gas removal is introduced. Finally, details about selected processes for acid gas removal that involve methanol are commented.

2.1. General Definitions

First of all, to start deepening into the processing strategies for acid gas removal, a definition of what an acid gas is must be given. This particular kind of gases conglomerates those that, in mixture with water, form an acidic solution. Among these, the most relevant in the gas industry are Carbon Dioxide (CO_2) and Hydrogen Sulphide (H_2S) [7, 8].

The criteria to define when a natural gas resource has considerable amounts of acid gas is not entirely fixed, but varies depending on several factors such as product and system specifications. Nevertheless, a general definition states that when volumetric compositions of H_2S and CO_2 are higher than 1% and 2%, respectively, acid gas removal is needed [5].

Acid gases have to be removed from the desired stream for several factors; among these product quality, safety and processing specifications. As mentioned before, these components have the capacity to form acidic solutions with water; another component typically present in the gas field. Therefore, the presence of these environments could compromise the integrity of the equipment

downstream [5]. Also, when LNG processing is aimed to occur upon further processing, the concentration of CO_2 has to be diminished to 50 ppmv due to risk of solids formation [5].

In order to meet safety requirements, H_2S concentrations have to be kept at low ppmv values, typically 4 ppmv [5]. This component is highly toxic and, when present in concentrations higher than 1000 ppmv, death occurs immediately [9].

In terms of product specifications, the presence of these components may alter the quality of the gas as fuel, particularly with the non-flammable CO_2, component that has to be removed to regulate the heating value of the gas [10].

2.2. Processing of Acid Gas

Once understood what acid gases are and the reasons for their removal, the processing is to be unraveled. Usually, in a gas processing plant, either onshore or offshore, the acid gas sector of the plant is located after the receiving and heavy hydrocarbon (HHC) condensates stages [11]. The latter is illustrated in Figure 2.1.

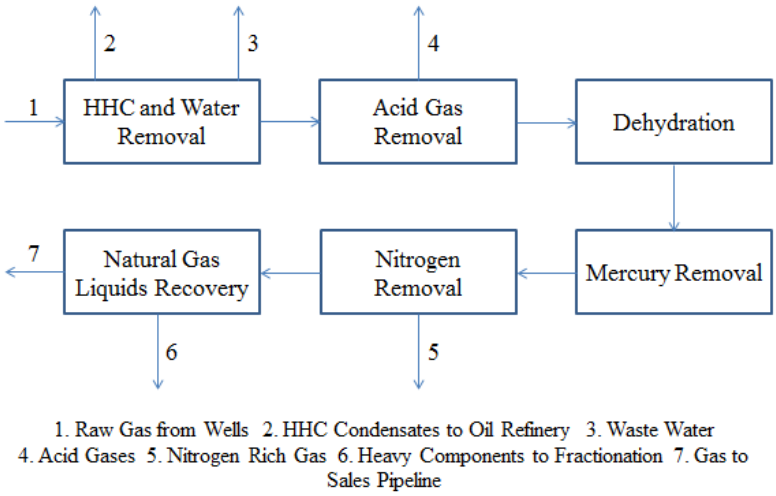

Figure 2.1. Simple Block Diagram of a Gas Processing Plant [11]

Many of the applications used in sour gas treatment involve solvents as agents to achieve the separation. The solubility of HHC into these solvents can be relatively high and, therefore, problems occur in terms of extra processing of the lean solvent in order to be correctly purified for recycling purposes [5, 8].

As mentioned before, processing conditions also canalize the removal of HHC prior to enter the sour gas treatment. Some of the processes that are used in sour gas treatment operate at temperatures relatively low (-30 to -80 °C for *Rectisol* process, e.g.) [8]. At these conditions, the HHC dew point will be surpassed; hence leading to the formation of a condensate undesired liquid phase downstream [11].

Following the line of thought mentioned above, sour gas treatment comes after the HHC removal. Inside of this process stage there are several alternatives to select. Figure 2.2 shows the most relevant processes relating acid gas removal [8]. Also, detailed explanations for many of these processes are included in Kohl's *Gas Purification* [12].

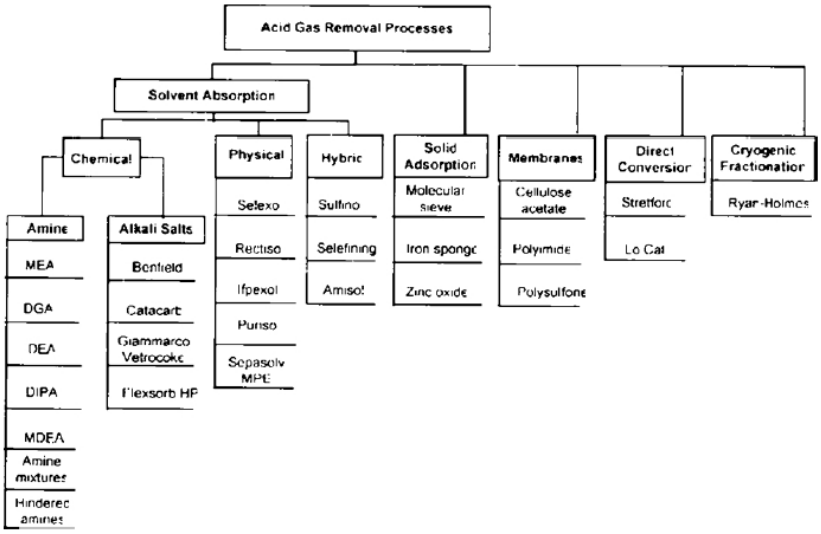

Figure 2.2. Acid Gas Removal Processes [8]

The selection of the process to be used depends upon a large number of factors; such as nature and concentration of the impurities present, the amount of heavy hydrocarbons in the stream to be processed, the PVT conditions of the gas, the selective versus total acid gas removal, product specifications, capital costs, environmental constraints, among others [8, 13].

Within these processes, solvent absorption ones are the most commonly used inside the gas the industry [5]. These have the common characteristic of utilizing a solvent as the agent to achieve separation. Mass transfer, physical solubility of the gases, chemical reaction and equilibrium principles are the fundamentals behind these separation processes [13].

This category of processes is preferred not only because they are widely developed and, therefore, the design options are by far tangible; but also because they are quite flexible in terms of plant

volume, product specifications, etc. [12] They represent two main challenges regarding costs: solvent circulation rate (affects the sizing and operation parameters of the plant) and the energy requirements of regenerating the solvent [8].

Among this group of solvent based operations there are two main subcategories of processes regarding the nature of the "separation driving force" present; these are chemical solvents, physical solvents and, in some cases, a mixture of solvents based processes [8].

As shown in Figure 2.2, there are several alternatives available for acid gas removal. Among them, adsorption, gas permeation and gas fractionation are the most relevant ones in terms of industrial presence [5]. Nevertheless, they will not be discussed as a topic of the project developed.

2.2.1. Processes based on Chemical Solvents

This family of processes is the one where the solvent "washes" the contaminant in the gas stream by means of chemical affinity and mass transfer principles. Among this group, amines and alkali salts are the most widely used solvents [5, 8, 12].

In order to begin addressing Amine Scrubbing processes, a definition of what an amine is must be given. An amine is a component that is produced from the substitution of an ammonia (NH_3) hydrogen atom for another aryl (aromatic) or alkanol (hydrocarbon) group. They will be primary, secondary or tertiary according to the number of hydrogen atoms that are substituted [14].

Absorption of contaminants with amines (amine scrubbing) follows two main steps. First, the contaminant present in the gaseous phase dissolves into the liquid phase (physical absorption); being the governing force in this step the partial pressure of the H_2S and CO_2 in the gas. Then, the dissolved contaminant (a weak acid) will react with the amine (a weak base) in an acid-base reaction [8].

Several options are present in terms of the amine to be selected. Among these, the most commonly used are Monoethanolamine (MEA), Diethanolamine (DEA) and Methyl-diethanolamine (MDEA) [5]. The following Figure 2.3 shows a typical amine gas treating process.

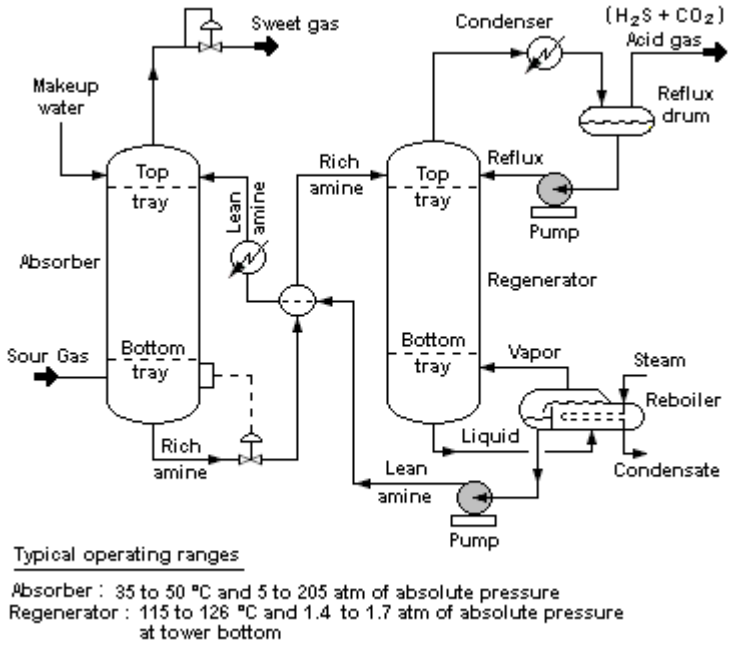

Figure 2.3. Process flow diagram of a typical amine process [15]

Among the factors that hinder the processing with amines are foaming, corrosion, degradation and oxidation. Common solutions to these problems are, respectively, introducing anti-corroding components, anti-foaming agents and placing the amine solutions with inert gases [5].

The other group of chemical based processes to be commented is that one including Alkali Salts Scrubbing. These are similar to the amine scrubbing ones and they recur to the use of alkali salts, such as potassium carbonate (K_2CO_3), to achieve the separation [8]. The process in question can be designed to require less energy demand for regeneration and smaller processing equipment in comparison to amine scrubbing, scenario where this alkali option might be selected [8]. A general scheme of this process for K_2CO_3 is shown in Figure 2.4.

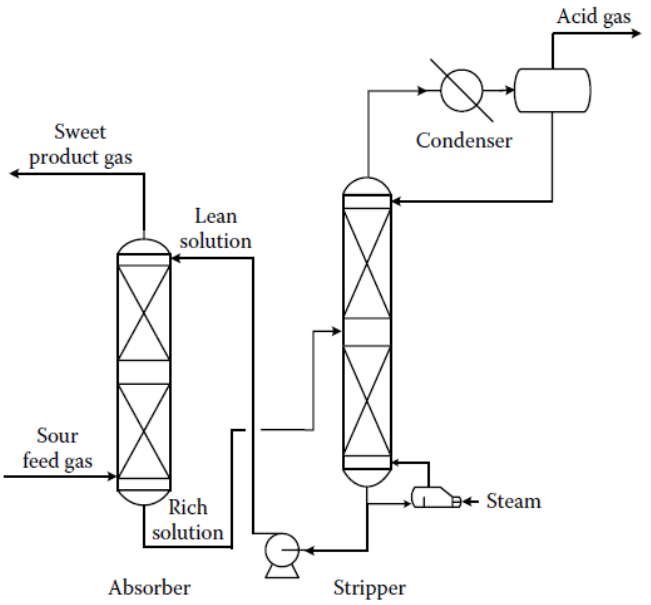

Figure 2.4. Process flow diagram for a hot potassium carbonate process [8]

2.2.2. Processes based on Physical Solvents

This category of processes has its fundamentals on the partial pressure of the contaminants within the stream to be processed. Being the driving force of the process, the higher these pressures the more the amount of contaminant that will be carried along with the solvent. In contrast with the amine solvent processes, the absorption takes place in one step: dissolution of the contaminant into the solvent liquid stream [5, 8].

Physical solvent based processes have several advantages that make them attractive alternatives. When the proper solvent is chosen, selectivity within CO_2/H_2S can be accomplished [8]. These processes are recommended when large amounts of acidic components are present in the gas source, this due to the fact that reduction to ppmv values can be achieved with these processes at low costs [5].

Also, heat regeneration is not needed in order to recover the solvent. This step is performed via successive expansions, stripping by a neutral gas or reboiling of the solution [5]. The amount of purification aimed to complete with the absorption will rule the way in which the solvent shall be recuperated; ranging from a simple flashing stage to complex designs with different pressure stages and operations [12]. A scheme of three different configurations of physical solvent processes, regarding the method to recuperate the solvent are displayed in Figure 2.5.

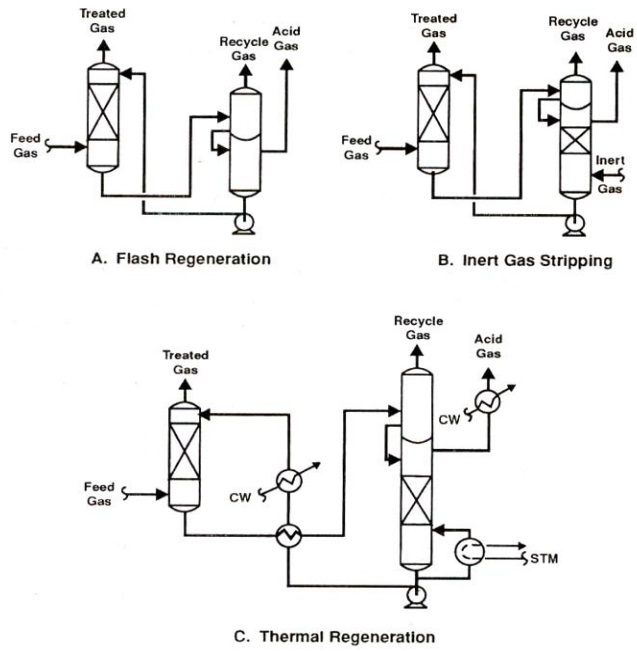

Figure 2.5. Different solvent regeneration configurations for physical absorption [12]

The main restriction associated with physical solvent processes is that one related to the absorption of heavy hydrocarbons along with the solvents used. Usually, the process is not recommended in those cases where these components make a significant amount of the stream to be treated; but if the studies point to the use of physical solvents regardless of the HHC content several alternatives are available [8].

Removal of the HHC components prior entrance to the absorption unit might be a viable option, this achieved through expansions and flashings stages that will generate condensates of these components [8]. Also, integrated processes can be utilized, such as the *Ipfexol*; where dehydration, HHC separation and acid gas removal occur simultaneously [12]. For further characteristics of this process, see section 2.3 of the current chapter.

Several processes have been design for physical solvents, such as *Rectisol, Selexol* and *Purisol*. Also, there is a family of processes called mixed physical/chemical solvents; where the solvent used is a mixture of components that is capable of seizing the advantages of each kind of processes. Among these, *Sulfinol* and *Amisol* are the most widely known ones [12]. A thorough list of physical solvent based processes has been taken from Kohl's *Gas Purification* and is shown in Figure 2.6.

Table 14-1
Physical Solvent Processes

Process Name	Solvent	Process Licensor
Simple Physical Solvents		
Fluor Solvent	Propylene carbonate (PC)	Fluor Daniel
SELEXOL	Dimethyl ether of polyethylene glycol (DMPEG)	Union Carbide
Sepasolv MPE	Methyl isopropyl ether of polyethylene glycol (MPE)	Badische (BASF)
Purisol	N-Methyl-2-pyrrolidone (NMP)	Lurgi
Rectisol	Methanol	Lurgi and Linde AG
Ifpexol	Methanol	Institut Français du Pétrole (IFP)
Estasolvan	Tributyl phosphate	IFP/Uhde
Methylcyanoacetate	Methylcyanoacetate	Unocal
Mixed Physical/Chemical Solvents		
Sulfinol	Sulfolane and DIPA or MDEA	Shell Oil/SIPM
Amisol	Methanol and secondary alkylamine	Lurgi
Selefining	Undisclosed physical solvent and tertiary amine	Snamprogetti

Figure 2.6. List of the most relevant physical solvent processes [12]

2.3. Processes that involve methanol as a solvent

As mentioned before, there are several alternatives to be selected within the physical solvent processing. Regarding the fact that

methanol is the solvent of study during this project a compilation of processes that involve this substance are presented. There are a small number of processes that use methanol purely as the absorption solvent, among these *Rectisol* and *Ipfexol*. Others, like *Amisol*, use this component in addition with other substances [12].

One of the main characteristic of these processes is their low temperature operation for the absorption step. Temperatures as low as -30 to -80 °C can be utilized in the processing, this due to the high vapor pressure of methanol; situation that will imply significant losses of solvent if operation occurred at higher temperatures. Also, low temperature operation is related to higher absorption of contaminants, given the fact that the solubility of CO_2 and H_2S behaves inversely against the temperature. The latter can be evidenced in Appendix D [5].

From the totality of processes available, two have been selected in order to deepen more into their steps and characteristics. These two mentioned are *Rectisol* and *Ipfexol*. The information presented for these processes is a good way of getting an image of the units and operating conditions of a methanol solvent based process, such as the one studied and structured during this project.

2.3.1. Rectisol Process

The *Rectisol* process, developed and licensed by Lurgi GmbH and Linde AG, is one of the main processes used for sour gas treatment in the syngas production. The process can handle the impurities related with the gasification of coal and heavy oil. Also, it is a good alternative to facilitate the dehydration and the prevention of hydrate and ice formation [12].

As mentioned before, the process operates at low temperatures due to the high vapor pressure of methanol and to the increase of solubility in methanol of the contaminants at these temperatures. This results in complex plants designs that imply considerable costs both in terms of construction and operation [12].

Concentrations of CO_2 and H_2S can be reduced to values as low as 1,5 and 0,1 ppmv; respectively. *Rectisol* process is also advantageous in terms downstream contaminant treatment; given the fact that is flexible in the adaptation to Clauss processing (Sulfurs treatment) and Enhanced Oil Recovery projects with CO_2 [16].

Depending on what product specifications are presented, the process can either be selective or not in terms of the contaminants being "washed". According to this, three configurations of the process results: a process that removes all the contaminants, a process that removes selectively one of the contaminants and a process that removes selectively each of the contaminants, resulting in two main outlet impurities streams [12].

A simple PFD of the process with selective treatment of CO_2 and H_2S for syngas production is presented in Figure 2.7. As many of the processing involving physical solvents, it follows four basic steps:

- A pretreatment stage; were the conditioning happens to meet downstream specifications. Heat exchanging units and flash vessels usually shape this stage.
- A contaminant removal step; where the absorption of the impurities occurs. In this case, it is divided in two subsequent steps: firstly a H_2S removal unit and then the absorption of CO_2.
- A regeneration stage; where the solvent is recuperated and returned to the respective absorption units.

- A downstream treatment stage, in which further processing such as HHC recovery, contaminant treatments occur, among others.

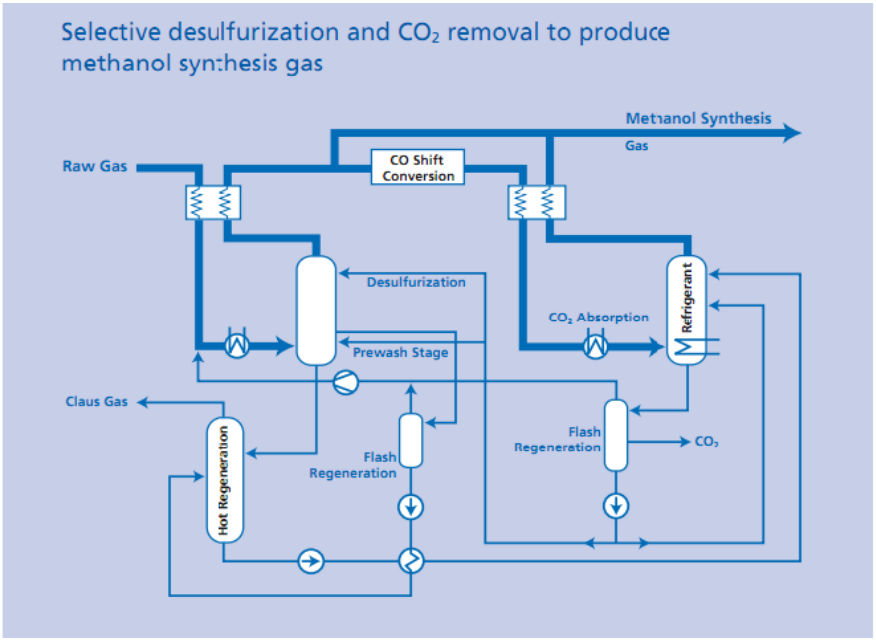

Figure 2.7. Simple PFD of a selective *Rectisol* process for Syngas production [16]

Additional information of the process can be found in Appendix D, this regarding typical processing conditions and flow schemes of the process.

2.3.2. Ifpexol Process

This process, as mentioned in previous content, belongs to the category of integrated processes. Methanol is used in three different ways within it: dehydration, natural gas liquids (NGL) recovery and

acid gas removal. It is further divided in two sub-processes: IFPEX-1 and IFPEX-2. The first treatment involves the pre-treatment before the acid gas removal: dehydration and heavy hydrocarbon condensation. IFPEX-2 involves the absorption stage and the recovery of the solvent [12].

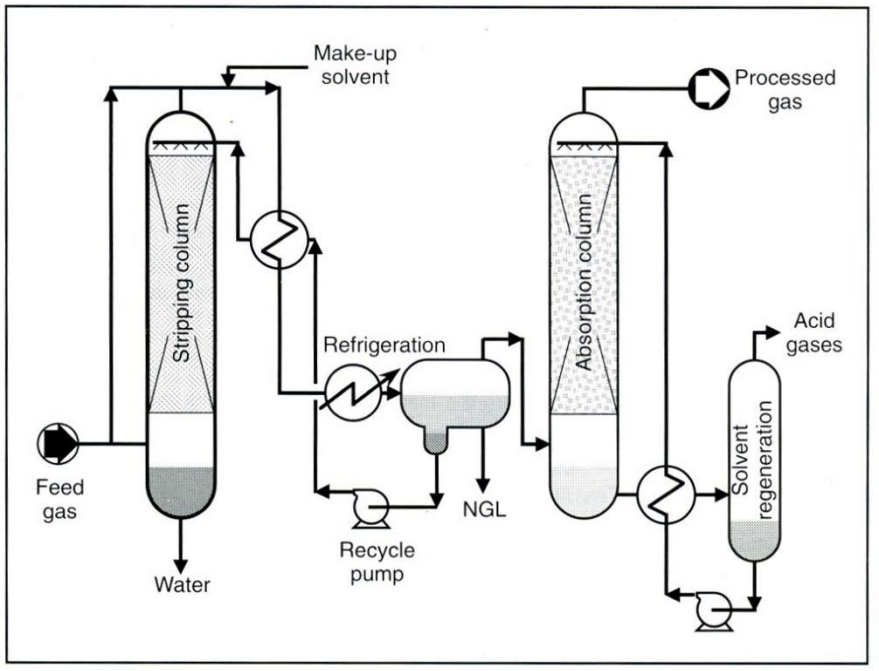

Fig. 7.31 *Ifpexol* process.

Figure 2.8. Simple flow diagram of *Ifpexol* process [5]

In Figure 2.8 a flow diagram of the process is displayed. The water stripping column has as feed a fraction of the natural gas feed and the recycle solvent; which is actually an aqueous solution of methanol with the water circulating inside the process. The majority of the water is removed in the bottoms, while the more volatile methanol goes through the heads with the natural gas and water remaining. One important fact to mention is that less than 50 ppmv

of the solvent is lost in the bottoms stream after this stripping process [12].

Then, the gaseous stream is subject to refrigeration and condensation, having three phases as products. The heaviest phase is composed of the aqueous solution of methanol to be recycled towards the stripping process. The other liquid phase corresponds with the NGL to be recovered and the gas one is mainly composed of light hydrocarbons, gaseous methanol and the contaminants. IFPEX-1 would correspond with these two latterly mentioned steps [5, 12].

Then, this rich gas stream is taken to the absorption unit. On the heads, the processed gas is obtained with concentrations of H_2S and CO_2 as low as 1% volumetric. On the bottoms a rich solvent stream is obtained and flashed. The resulting flashing streams correspond with the lean solvent to be recycled to the absorption unit and the acid gases. These steps are included within the IFPEX-2 part of the processing [5, 12].

3. THE NATURAL GAS FEEDING STREAM

The following section of the thesis addresses the main characteristics of the gas stream to be treated, as well as some quality specification given. Also, information about the source of the feeding stream is introduced.

3.1. General Information

One of the most important steps within the project was the definition of the natural gas stream to be treated. As a suggestion from the tutors, a rich gas stream was selected from the Snøhvit offshore field, located approximately 140 Km northwest of Hammerfest, a Norwegian city within the northernmost department of the country, Finnmark [17]. Figure 3.1 illustrates the localization of the field within Norway.

Figure 3.1. Localization of Snøhvit field within the Barents Sea [18]

The first major subsea development in the Barents Sea, Snøhvit has an accumulation of natural gas of 193 billion standard cubic meters (bscm), 113 million barrels of condensate and 5.1 million tons of NGL. The gas extracted from this field is considered to have

enough acid gas contaminants to be subject of sour gas treatment [17].

Once acid gas removal has been accomplished, the purified stream goes into further processing; being the most relevant of these the production of LNG. Each year from Snøhvit, approximately 70 LNG tanks are shipped; this following an annual production of around 5.75 bscm of LNG [17].

On the other hand, the CO_2 produced from the plant processing is significant; compromising then the emissions limits permitted. Therefore, carbon capture and storage (CCS) strategies are used to re-inject the contaminant obtained, hence reducing the environmental impact of the processing [17].

The compositional chart for the feed stream selected is presented in Table 3.1.

Table 3.1. Composition chart of the natural gas feed stream.

Component	Molar Fraction
Methane (C1)	0,830
Ethane (C2)	0,054
Propane (C3)	0,025
Isobutane (i-C4)	0,004
n-Butane (n-C4)	0,007
Pentane plus (C5+)	0,005
Carbon Dioxide (CO_2)	0,050
Nitrogen (N_2)	0,025

The volumetric flow rate of the stream is 20 MSm^3/day (million standard cubic meters per day). The feeding pressure and temperature conditions are, respectively, 10 °C (283,15 K) and 70 bara.

3.2. Considerations about the gaseous stream

Some considerations have to be taken from the composition chart of the feed stream before continuing with further contents. First of all, this stream does not correspond with the actual natural gas stream extracted directly from the reservoir. The absence of key substances like water indicates that this stream is located somewhere within the treatment of the process, probably after a dehydration unit.

Moreover, the absence of H_2S among the components indicates that only CO_2 is the acid gas contaminant to be addressed in further contents (Chapter 5). In addition to the actual lack of this component in the Snøhvit resources, the absence has also as objective the reduction of the amount of information handled within the project; focusing mainly in the CO_2 as the acidic contaminant.

3.3. Other specifications related to the feed stream

Along with the stream compositions, some additional information was specified; this related with restrictions for downstream processing.

In terms of the maximum concentration of CO_2 permitted before entering to the LNG treatment, a value of 50 ppmv in the clean gas stream was set up as maximum (Chapter 2).

On the other hand, in order to utilize the CO_2 removed for CCS; re-injection specifications were given. There are related to maximum amounts of methane and nitrogen permitted, being both values 2 % on a molar basis.

4. SIMULATOR AND THERMODYNAMIC MODELS

4.1. The Simulator Package: Pro II with Provision

In order to be able to predict behaviors and parameters for any system a simulation tool has to be selected. There is a wide range of simulator packages inside of the process design industry [19] and the selection of which one might be more appropriate for any given problem is widely related with the nature of the system, as well with its conditions of operation.

Pro II with Provision, a program developed by SimSci-Esscor, is presented as an alternative to cope with the simulation of chemical engineering related plants. This package belongs to the Steady State Process simulators and it is mainly used by process engineers inside of the petroleum, natural gas, solids processing and polymer industries [20].

Regarding the natural gas system studied during the length of this project, a simulator capable of modeling acid gas scenarios was needed. Pro II possesses an extensive list of components, in which both acidic (CO_2 and H_2S), inert (N_2) and hydrocarbon (Methane, Ethane, etc.) components are contemplated [21]. Also, the simulator presents a set of thermodynamic models that are recommended to represent systems with natural gas mixtures in presence of polar components, such as the methanol solvent used in for the absorption stage within acid gas removal process discussed [21].

Likewise, the simulator presents a wide range of unit operations associated with the processing scenario in question. This opens the possibility of representing the actual system in a more accurate manner; being feasible to simulate absorbers, heat exchangers, flash

drums, expanders and further equipment present in a typical sour gas treatment plant [21].

Process simulators are useful alternatives to design and explore developing or existing projects; giving the option of changing parameters and studying their influence in the system. All of these can occur without the need of materializing the system or having to re-build it in case of evaluation after previous operation [21].

Nevertheless, the use of these tools implies some disadvantages; such as obtaining computational calculations that in practice are not possible to achieve. Also, several "default" inputs of the program limit the similarity of the process against reality. In the particular case in study, irregularities inside the absorption unit may occur for certain operation parameters, these tied with tray efficiencies or internal calculations that are not contemplated within the input parameters, e.g. [21]

Other limitation related with the use of simulators for modeling real systems is that one associated with the accuracy of the data obtained. Despite presenting Equation of States (EOS) that adjust to specific systems, such as sour gas streams, the model can present deviations from the data presented in the literature, the latter assumed as the actual one. Computations regarding literature and simulated must be done in order to measure the amount of uncertainty that is being handled with the model selected [21].

4.2. The SRK-Panagiotopoulos-Reid Modified EOS

The thermodynamic set used to describe the system is that one corresponding with the Soave-Redlich-Kwong EOS (1972) [23] modified firstly by Panagiotopoulos-Reid (1986) [23] and then by SimSci-Esscor; resulting in a model addressed as SRK-

Panagiotopoulos-Reid Modified and included in the thermodynamic data options of the simulator. The selection of this modified EOS version was taken, firstly, in accordance to what the User's Manual of the program recommends for mixtures as the one studied in this project.

4.2.1. The Soave-Redlich-Kwong Equation

To describe the model presented by the simulator, a set of previous concepts have to be introduced. First of all, the Redlich-Kwong EOS is displayed:

$$P = \frac{R \cdot T}{\vartheta - b} - \frac{a(T)}{\vartheta \cdot (\vartheta + b)} \tag{4.1}$$

This cubic equation, as all EOS do, relates pressure (P) in terms of the absolute temperature (T) and molar volume (ϑ). The universal gas constant (R) is part of this equation and its value is related with the set units used for the PVT properties; for SI units, the value is 8.314 J*mol^{-1}*K^{-1} [24]. The *a(T)* and *b* terms in the EOS are related with the substances present and there are expressions to calculate them. To begin, the *a(T)* shall be addressed. This term was introduced as a constant by Redlich-Kwong (1949), with no temperature sensitivity. The expression for this constant corresponds with the following one:

$$a(T_c) = 0{,}427481 \cdot \frac{R^2 \cdot (T_c)^2}{P_c} \tag{4.2}$$

The latter equation is given in terms of critical values (T_c and P_c); which are characteristics for each substance. Soave (1972) [23] added a temperature sensitive function to the expression known as α:

$$\alpha(T) = [1 + M \cdot (1 - T_r{}^{0,5})]^2 \quad (4.3)$$

Where T_r is the reduced temperature and M is polynomial in function of the acentric factor (ω), the latter a parameter characteristic to each substance. Both terms are defined in the following equations, respectively:

$$T_r = \frac{T}{T_C} \quad (4.4)$$

$$M = 0{,}480 + 1{,}574 \cdot \omega + 0{,}176 \cdot \omega^2 \quad (4.5)$$

The expression for the *a* term, including the Soave addition, ends up as stated in equation (4.6).

$$a(T) = \alpha(T) \cdot a(T_c) \quad (4.6)$$

Only the term *b* is to be developed. This term is a constant relative to the substance in question and it is expressed in term of critical properties.

$$b = 0{,}086641 \cdot \frac{R \cdot T_c}{P_c} \tag{4.7}$$

4.2.2. Multicomponent modifications for the SRK EOS: Mixing rules.

When the system in question is a multicomponent mixture, the accuracy of the results calculated when using the SRK EOS not only relies with modifying the parameters to make them temperature sensitive, but also in the mixing rules used to predict them [23].

Several alternatives in mixing rule terms have been proposed to adjust the EOS to multicomponent systems, being the most commonly used the quadratic mixing rule [23]. Regarding the latter, the *a* and *b* parameters for the mixture are expressed in equations (4.8) to (4.10).

$$a = \sum_i \sum_j x_i \cdot x_j \cdot a_{ij} \tag{4.8}$$

$$a_{ij} = \left(a_i \cdot a_j\right)^{0,5} \cdot (1 - k_{ij}) \tag{4.9}$$

$$b = \sum_i x_i \cdot b_i \tag{4.10}$$

In the above equations, the *x* corresponds with the fraction of a component within the mixture. The k_{ij} is known as the interaction parameter and it is related with the binary interaction of the component *i* against component *j*. This mixing rule works

accurately for mixtures of components that are non-polar or weakly polar. In order to meet better results for mixtures containing polar components, Panagiotopoulos and Reid (1986) [24] proposed a new expression for the a_{ij} term; introducing a k_{ji} term that contemplates asymmetric interactions between one or more polar components. If the value k_{ji} is equal to the k_{ij}, the following equation is simplified into equation (4.9).

$$a_{ij} = \left(a_i \cdot a_j\right)^{0,5} \cdot \left[\left(1 - k_{ij}\right) + \left(k_{ij} - k_{ji}\right) \cdot x_i\right] \qquad (4.11)$$

Even though the Panagiotopoulos-Reid modification is useful to represent highly polar systems, the expression stated in equation (4.11) is only used for binary systems [24]. In order to extend the SRK-Panagiotopoulos-Reid EOS to multicomponent polar mixtures, SimSci-Esscor modified the a_{ij} term [24]:

$$a_{ij} = \left(a_i \cdot a_j\right)^{0,5} \cdot \left[\left(1 - k_{ij}\right) + \left(k_{ij} - k_{ji}\right) \cdot \left(\frac{x_i}{x_i + x_j}\right)^{cij}\ \right] \qquad (4.12)$$

Where C_{ij} is another empirical constant that measures interaction between components. In practice, the simulator encloses the calculation of the *a* term in an empirical function that has as inputs three constants (*C1*, *C2* and *C3*), the reduced temperature (*Tr*) and the acentric factor (ω). Then, the mixing rule is used to calculate the interaction terms. All of the latter constants and properties are extracted from the simulator property data bank [21].

4.3. Accuracy of the Thermodynamic Model

Once the model has been presented and selected, it must be tested in order to be sure that the results obtained are accurate enough. To achieve this, a strategy was followed to compare experimental researched data and simulated data.

First, the research data was collected. To narrow down the systems to look upon the data, the mixture was partitioned into three binary systems, always following the parameter solvent vs. one of the main components of interest within the mixture. The systems for which thermodynamic data was found are Methanol-CO_2, Methanol-CH_4 and Methanol-H_2S. The equilibrium data for these systems is presented in Appendixes A, B and C. An example of the data compiled is shown in Figure 4.1 for the Methanol-CO_2 system at T=233,15 K.

An important consideration to be noted is that the data presented only regards compositions for the liquid phase. The systems simulated present gaseous fractions close to 1 and therefore, the simulator approximates the calculations always to this value; being then unnecessary to report this values.

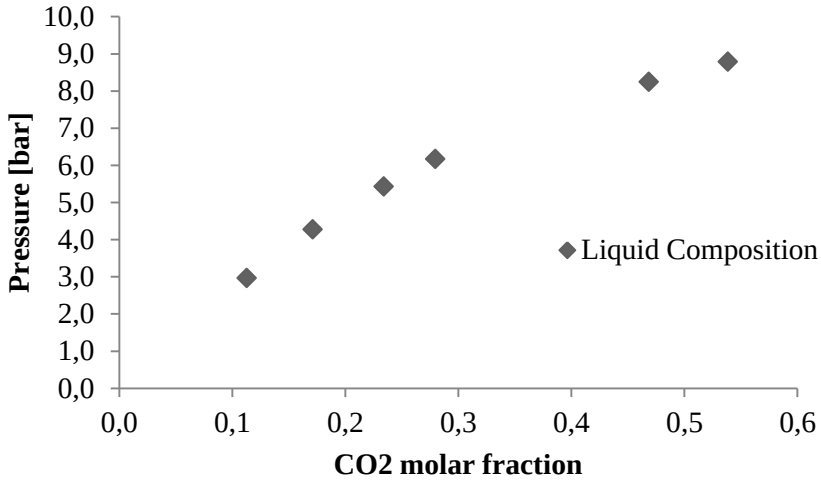

Figure 4.1. Methanol-CO_2 system equilibrium literature data at T=233,15 K.

4.3.1. Simulation of the literature data

The procedure followed to achieve the simulation of the literature data began with the selection of an appropriate feeding for each binary mixture to be studied. First, an equilibrium curve of the kind pressure vs. composition at a fixed temperature was constructed for each of the data table collected. Then, the amount of methanol to be fed was changed in order to assure that, at the simulating conditions, the system will guarantee the presence of two phase behavior, i.e., that the feeding point was inside of the equilibrium envelope.

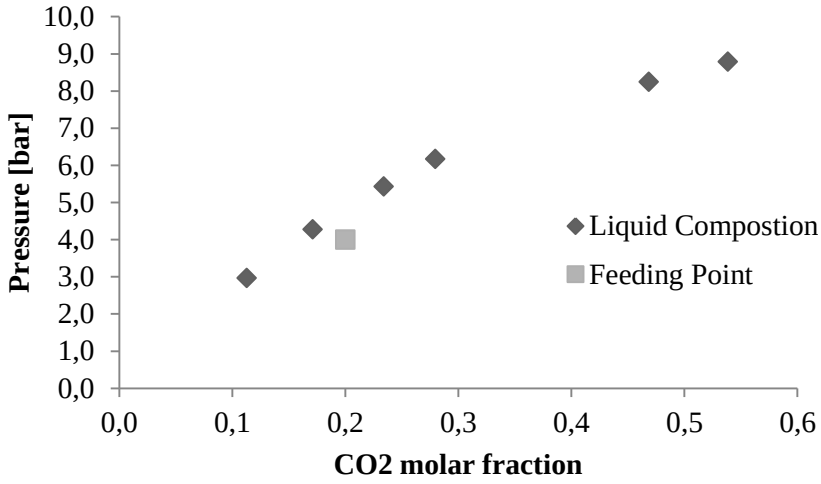

Figure 4.2. Example of a feeding point location at an operating point of 4 bara. Methanol-CO_2 system at T=233,15 K.

As shown in Figure 4.2, if simulating at a pressure of 4 bara, the feeding stream has to have a CO_2 molar fraction of, approximately, 0,2. If the mixture fed has a significant lower CO_2 molar fraction (0,1; e.g.), the system will not present two phase behavior. This simple analysis was made for every set of pressure and temperature simulated.

Then, a simple Process Flow Diagram (PFD) was constructed to achieve the equilibrium conditions and then flashing operation for each methanol-solute system simulated. The PFD consisted of only two operation units. The first one, an isothermal mixer where the solvent and the solute where put in contact. The feeding streams to this mixer where set up at standard conditions, these meaning at a temperature of 273,15 K and a pressure of 1,0132 bara [24].

As can be observed on the Appendixes A, B and C; the literature data is presented for every system at a fixed temperature; for which

different pressure values give the compositional equilibrium data. Therefore, the mixer outlet pressure was set up to be equal to each of these pressure values for every given T; these restriction being done in order to guarantee that the point (Pressure and Temperature) to be simulated corresponded exactly with the point reported on the literature.

After achieving the desired methanol-solute stream, the latter was input into a Flashing Drum. This unit was assumed isobaric and the operating outlet temperature was that one of the set of data to be compared. After the flashing, two streams where obtained corresponding with the two phases present: liquid and vapor ones. Figure 4.3 shows the Pro II flowsheet constructed for this simulation.

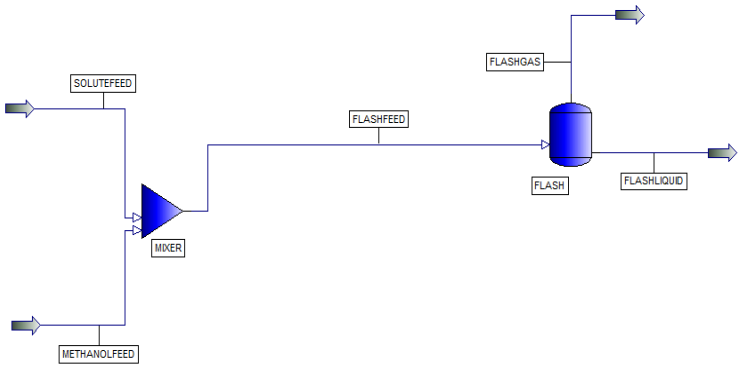

Figure 4.3. Pro II simulation flowsheet for the researched data vs. simulated data comparison.

The compositions of solute in question for each system (set of P and T values for each solute) were tabulated and presented in Appendixes A, B and C. An example of these results is presented in Figure 4.4

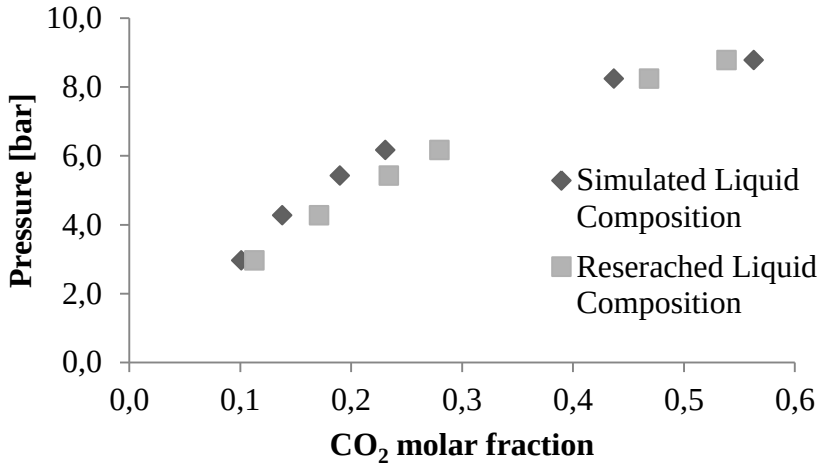

Figure 4.4. Simulated and literature results for Methanol-CO_2 system at 233,15 K.

4.3.2. Simulated data obtained vs. researched equilibrium data

Once the simulations were done, the data obtained had to be compared with that one extracted from the literature. In order to do so, a percentage error between these two set of values was calculated for each point. The expression associated with this error is stated ahead:

$$e_{\%} = \frac{V_r - V_s}{V_r} \cdot 100 \tag{4.13}$$

Where $e_{\%}$ corresponds with the percentage error between V_r (literature researched value) and V_s (simulation obtained value). Both values represent the molar fractions of the solute within the Methanol-solute (CO_2, H_2S and CH_4, respectively) mixture. A thorough list of these results is presented, along with the before

mentioned simulated and researched values, in Appendixes A, B and C. An example of this list is presented below (table 4.1) for the Methanol-CO_2 system at 233,15 K.

Table 4.1. Results for the Methanol-CO_2 system at 233,15 K.

Reference	Pressure	CO_2 liquid mole fraction		Percentage Error (X)
	[bar]	Literature	Simulated	%
Weber et al. (1984)	2,960	0,113	0,101	10,619
	4,272	0,171	0,138	19,440
	5,427	0,234	0,190	18,803
	6,167	0,280	0,231	17,441
	8,239	0,469	0,437	6,743
	8,781	0,539	0,563	-4,530

To have a better image of the dispersion of the data in comparison with the literature data, the results have been presented in graphs (Figures 4.5 to 4.9) where the "Y" axis represents the percentage of deviation from the literature (0%) and the "X" axis corresponds with the different pressures inside the range of the data simulated.

Figures 4.6 to 4.9 include the comparisons between the literature and the simulated data at the set of temperatures and pressures stated in the researched points for each system. Figure 4.5 shows information regarding the comparison of data for a specific temperature (233, 15 K) for the Methanol-CO_2 system.

Also, other fact to be noted is the selection of the system Methanol-CO_2 at 233,15 K as an example throughout previous contents. This selection lies within the frame of the temperature upon which the sour gas treatment unit is operated. In addition, Figure 4.6 and Figure 4.7 are also discrete in terms of the temperature range that is displayed. In Figure 4.6, a range of temperatures (from 227,9 K to

253,15 K) was selected in order to make easier the observation of the simulator behavior around the temperatures that were studied in the absorption unit analysis (from 223, 15 K to 253,15 K). Further information regarding the latter contents is included in Chapter 5. The rest of the literature temperatures for the Methanol-CO_2 system are displayed in Figure 4.7.

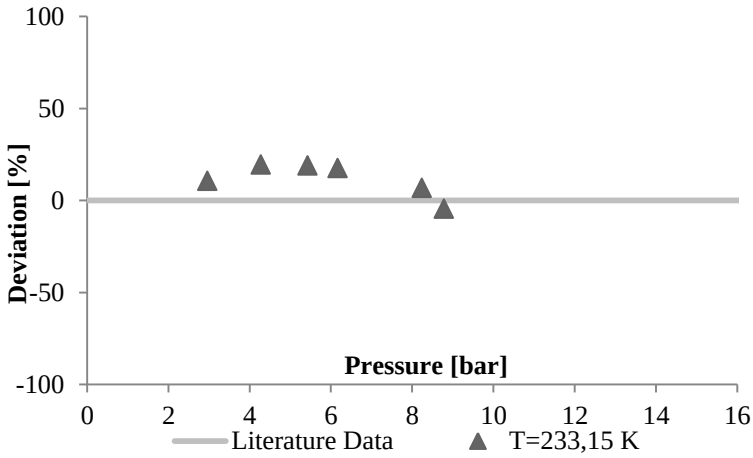

Figure 4.5. Percentage of deviation of simulated data vs. literature data for the Methanol-CO_2 system at 233,15 K.

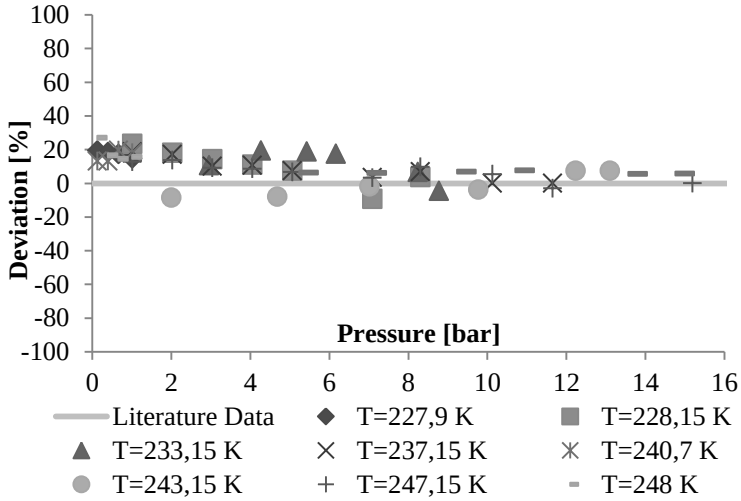

Figure 4.6. Percentage of deviation of simulated data vs. literature data for the Methanol-CO_2 system inside the simulated temperatures

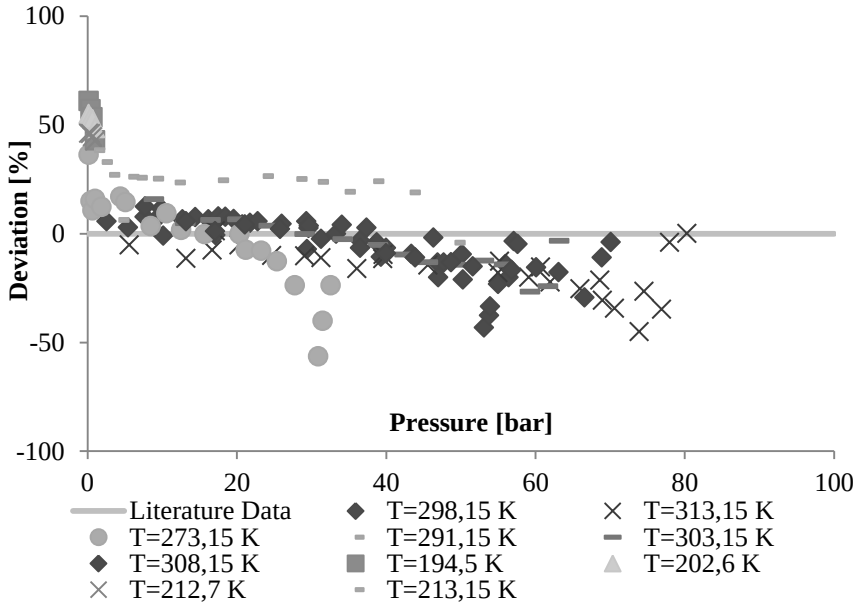

Figure 4.7. Percentage of deviation of simulated data vs. literature data for the Methanol-CO_2 system outside the simulated temperatures

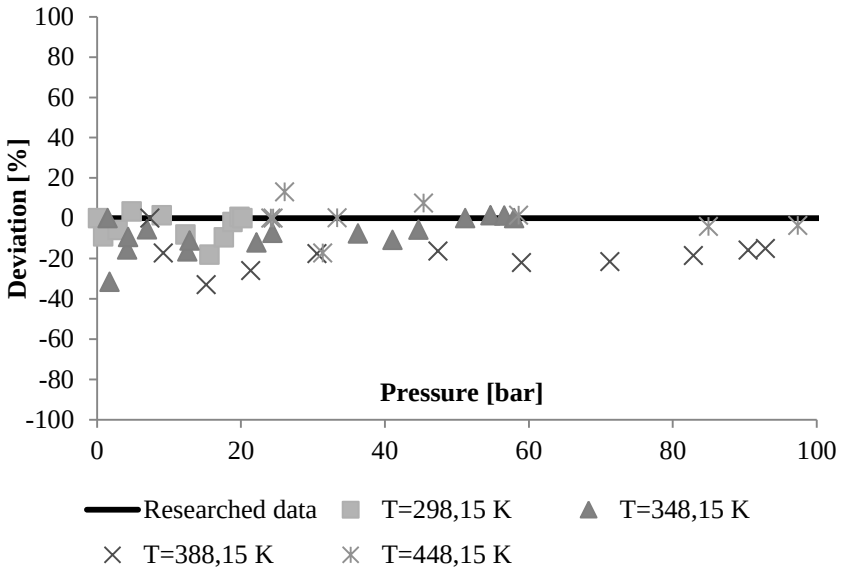

Figure 4.8. Percentage of deviation of simulated data vs. literature data for the Methanol-H_2S system

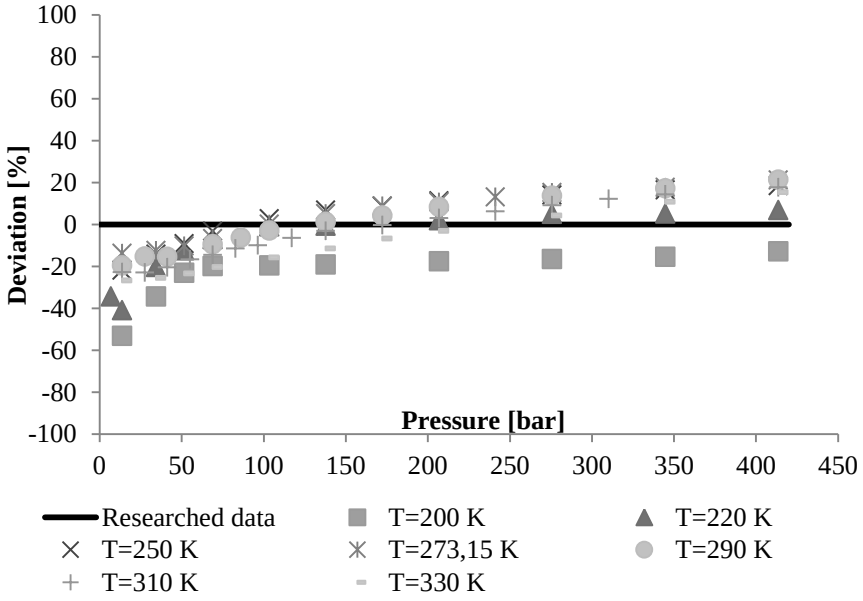

Figure 4.9. Percentage of deviation of simulated data vs. literature data for the Methanol-CH_4 system

4.3.3. Methanol-CO_2 system analysis

As the main contaminant component analyzed and discussed within the project (see Chapter 3), the relevance of a thermodynamic set that could represent accurately the Methanol-CO_2 system becomes evident.

The dispersion of the percentage errors between the thermodynamic simulated and researched data for this system was considerable. While some of the results obtained are almost identical to the reported ones (less than 5% deviation), values as high as 60,894 % are evidenced (T=194,5 K and 0,133 bar. Appendix A-1).

A general occurrence of high deviation values was observed at the extremes of the pressure range for each temperature. These points, usually, corresponded with the boundary limits of the equilibrium (0 and 1 molar fraction of CO_2). These values are related with the complete absence or presence of a component in a mixture, values that are impossible to reach through calculations since they are mathematical limits. This means that, e.g., to achieve the extreme where no fraction of CO_2 is present; the amount of the other component (in this case Methanol) should be taken to values appreciably infinite against the CO_2.

The theory behind this statement lies with the concept of infinite dilution, which corresponds with the state where a component in mixture with others is dissolved to the point where all its molecules are dissociated [25]. Such state is impossible to reach and, therefore, the simulator has to recur to extrapolations and other calculations that contribute with the deviation between researched and simulated values. Furthermore, the measurement of the experimental literature data is affected as well by this restriction. All of these are substantial enough that, when summed up, a significant amount of error is obtained for these values.

In closer look to the range of temperatures selected (Figure 4.8), the higher deviation observed (36,91 %) is that for the operation point of T=248 K and 0,133 bar (Appendix A-12). Once more, this point corresponds with the lowest pressure value for this mixture; following the tendency stated above. When taking a glimpse to Figure 4.5, the highest value corresponds with 19,440 % at 4,272 bar (Appendix A-7).

Deviations around 20 and 30 % are significant enough to reject the utilization of a model, but the reality is that these errors are associated with P-T points that are far located from those used in the simulations presented in Chapter 5. The pressures handled in the sour gas treatment are around the 70 bar. At these pressure, the highest deviation value is -17,166 % (Appendix A-20); this occurring at an operating temperature of 313,15 K; located afar from the highest temperature (253,15 K) simulated for the absorption unit (Chapter 5).

The outcome is that for the range of temperature selected while simulating the Methanol-CO_2 system the simulator calculates with sufficient accuracy; the deviation reported always below the 10 % value. So, for the conditions simulated, this margin of error is easily acceptable and can become acquainted to the study.

4.3.4. Other systems analysis

In addition to the Methanol-CO_2 results commented above, mixtures of the alcohol with hydrogen sulphide and methane were also studied. The results for these mixtures where tabulated and presented in Appendixes B and C, respectively. As done for the CO_2 mixture, these results were plotted and shown in Figures 4.8 and 4.9, respectively.

The behaviors observed for CO_2 are, approximately, followed as well for these components. In the case of methane, the errors are larger while approaching lower pressure values, as can be seen in Figure 4.9. The highest value for the set of comparison for this component was -53,15 % at 13,789 bar and 200 K (Appendix A-25). On the other hand, for the H_2S values the highest reported is -33,122 % (Appendix A-23) at 15,20 bar and 388,15 K.

Both in terms of pressure and temperature these peak values are, as in the case of CO_2, located outside the vicinity of the operation points studied (Chapter 5). For the equilibrium with H_2S, no data was found for the temperatures studied.

Nevertheless, the lower the temperature, the better the results for this component; situation that can be evidenced both in Figure 4.8 and in the Appendix B. This component was not simulated in further operations since the feeding stream analyzed comes from a H_2S free source. So, the limitations imposed by the deviations affiliated to this component can be dismissed henceforth.

Focusing on methane, the errors reported around the 70 bar operation point are always lower than 10% for the temperatures selected within the further sour gas study (Chapter 5). As stated before, this margin of uncertainty is easily acceptable to carry on with.

4.4. Further Work: considerations about the simulator-thermodynamics set

In order to conclude about the accuracy of the calculations being done with the simulator, some further considerations have to be done. First of all, the system in reality to be simulated is a

multicomponent mixture with several other substances apart from methane, carbon dioxide and methanol. The previous comparisons where done by the discretization of the system into binary mixtures and, in addition, binary mixtures of only two of the total components with the alcohol solvent.

The selection of these two components (methane and carbon dioxide) relies on the fact that methane is the component present in the biggest proportion in a natural gas stream (Chapter 3) and CO_2 is the goal contaminant to be removed; reason why its behavior should be carefully observed.

To have a better image of the deviation of the system while being modeled as a whole with the simulator, data from the multicomponent mixture should be provided and compared. Also, a different alternative is to present results for all combinations of binary components; i.e., extending the comparisons to ethane-methanol, ethane-methane, carbon dioxide-ethane, etc.

5. PROCESS SIMULATIONS

5.1. Building up the processing to be simulated

In previous sections of the report, fundamental information has been provided in order to construct a simulation flow sheet for an acid gas removal process. To begin with the sketching of the processing, a simple block diagram of an acid gas removal facility is illustrated in Figure 5.1.

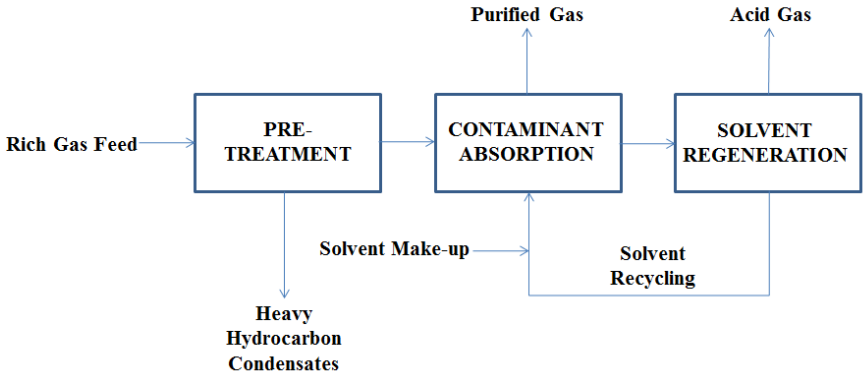

Figure 5.1. Basic block diagram of an acid gas removal process

The three steps shown in Figure 5.1 are common stages within a sour gas treatment process. Each step includes particular equipment and operation conditions in accordance to the characteristics of the plant design. In order to have sufficient information to construct a complete simulation of this scheme, a detailed study for each stage had to be done; starting from the inner absorption unit to the outer

stages. In the following sections of the text, details about this strategy will be presented.

5.2. Definition of the Absorption Stage

As the main unit operation in acid gas removal, this step of the process was addressed firstly in the simulation analysis. In this section, the incoming gaseous stream is subject to absorption with a methanol stream that washes out the contaminants; resulting this in two streams: a solvent rich in contaminants and a purified gaseous stream. This separation occurs inside of an absorption tower.

5.2.1. Input parameters: variables and assumptions

To begin with the explanation of the input parameters selected to design the absorption unit, these are presented in Table 5.1.

Table 5.1. List of input parameters and assumptions for designing the absorption unit

Parameter	Values and/or descriptions
Type of unit	Absorption tower with trays without reflux and reboiler
Feeding trays	Solvent stream: top tray. Gas stream: bottom tray
Number of trays	Variable. From 2 until 10 with a step of 1 tray. From 10 until 20 with a step of 5 trays.
Feeding compositions	Gas stream: 95 % CH_4 / 5 % CO_2 (molar basis). Solvent stream: 100% Methanol (molar basis)
Feeding flow rates	Gas stream: 20 000 sm^3/day (37,179 Kg-mole/h) Solvent stream: Variable. From 2 until 100 Kg-mole/h with a step of 2 Kg-mole/h.

Table 5.1 continued	
Feeding Temperature	Gas stream: Variable. 10 K less than the temperature of the solvent stream. Solvent stream: Variable. From 223,15 K to 253,15 K with a step of 10 K.
Feeding pressure	Gas stream: 70 bara Solvent stream: 69,5 bara ΔP Tower: 0,5 bara

Once presented this list, commenting about the parameters selected follows. Referring firstly to the type of unit utilized, a tray column was selected. Even though this configuration is not unusual within absorption columns, it is quite common to find schemes with packed fillings [26]. As selecting a specific filling to the column would add an additional degree of uncertainty to the simulation; the tray option was preferred. In Figure 5.2 a scheme of an absorption tower is displayed. To the left is a longitudinal façade of the column (either tray or packed one), while several filling options are presented to the right of the image.

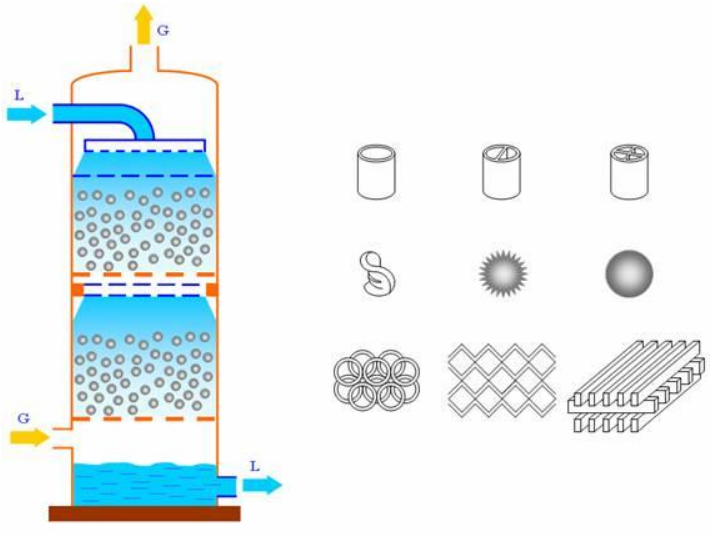

Figure 5.2. General Absorption Colum Outlook

Regarding the feeding trays, as the column was designed without reflux and reboiler, they had to be located in the extreme trays in order to guarantee phase contact along the column.

The number of trays inside the column was varied from 2 (the minimum value allowed by the simulator) until 20; the latter being the last value for which the column converged when running the flow sheet.

When defining the compositions for the feeding streams, some simplifications were made. First of all, as the pre-treatment to remove HHC is accomplished before this stage of the processing; the gas stream was reduced to the contaminant (CO_2) and to the main hydrocarbon (CH_4); this to avoid the formation of a hydrocarbon phase at the temperature of operation. The solvent composition of pure methanol was also affected for the lack of parallel interchange with further stages of processing, as it should be slightly "contaminated" with other components due to recycling from the regeneration step.

In terms of the flow rates simulated, these had to be scaled down a thousand times in comparison with the given value (Chapter 2); because of non-convergence of the simulator at these high flow rate values. This assumption affect, mainly, the physical design of the tower (diameter, e.g.) [26]; a section of the designing that was not addressed during this project. The solvent rate was, as done with the trays, from a low value up to an elevated one; this is order to have a range of results representative enough.

When choosing the range of feeding temperatures, this was set upon the typical operation range of *Rectisol* for the solvent temperatures (Chapter 2). At temperatures lower than the minimum value set (223,15 K) the convergence of the column is lost. In terms of the temperature difference between the feedings (10 K), this was a recommendation from the tutors for typical operation parameters for

this kind of units. The pressure values selected also follow a proposal of this kind; while the 0,5 bar pressure loss along the tower can be found within rules of thumb in the literature [26].

5.2.2. Results obtained

As can be observed from the previous section, three main design parameters were selected as variable in order to find the configuration most adequate for the system. The procedure used to simulate these three variables simultaneously is the following one:

- Fix the inlet temperatures inside the range as mentioned in Table 5.1.
- Fix the number of trays to one of the values within the range (From 2 until 20 trays).
- Vary the flow rate of methanol from 2 until 100 kg-mole/h.
- Report results.
- Repeat for a new number of trays.
- After having covered all number of trays range, repeat for a new temperature value.

The results calculated for each iteration were molar compositions of CO_2 and Methanol in the overhead of the column and compositions of CO_2 and CH_4 in the bottoms.

In order to decide which set of results was going to be selected as the operation parameters for the process, a specification had to be introduced. Parting from the restriction of CO_2 composition within the purified gas stream after the absorption step mentioned in Chapter 2 for LNG related processing, the 50 ppmv value was defined as the specification needed.

The first step done corresponded with the plotting of the CO_2 fraction within the gaseous stream (heads) vs. the solvent flow for each number of stages at a fixed temperature. An example of these graphs is presented in Figure 5.3 for a solvent temperature of 233,15 K.

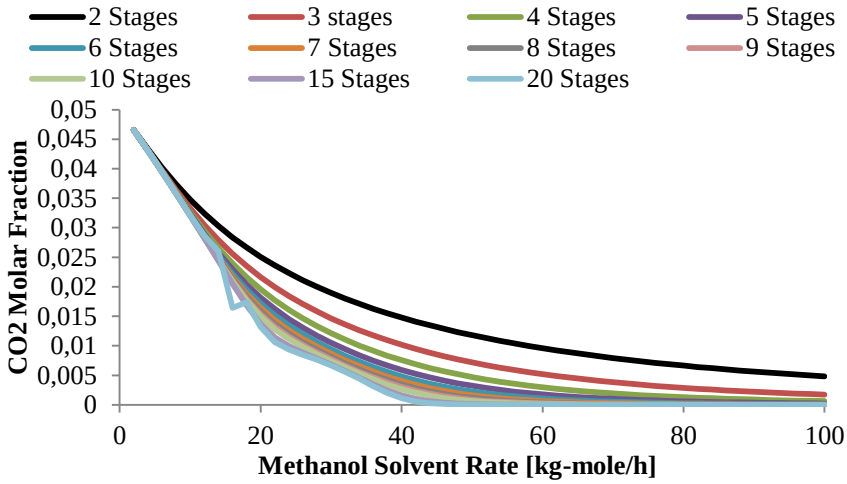

Figure 5.3. CO_2 molar fraction profiles for the absorption tower at a solvent temperature of 233,15 K

The 50 ppmv value was located in the "Y" axis; this to be able to identify the set of solvent rates at this value. To make the leture of this flow rates easier, a zoom around the 50 ppmv constant line was made and shown in Figure 5.4.

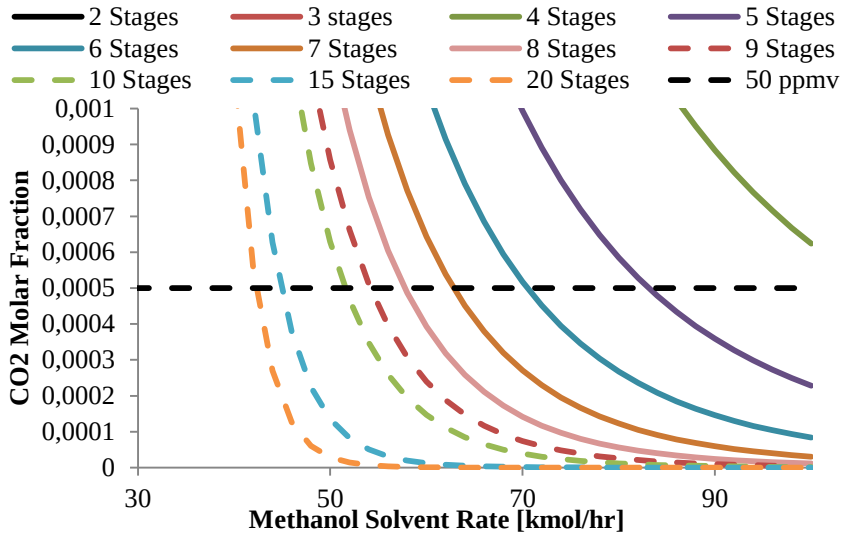

Figure 5.4. CO_2 molar fraction profiles for the absorption tower at a solvent temperature of 233,15 K (50 ppmv Zoom)

With the flow rate data collected that satisfies the CO_2 outlet restriction, a column profile curve was constructed for each solvent temperature. An additional constraint regarding the molar fraction of CH_4 carried with the rich solvent stream (bottoms) was set; this was done in order to control and minimize the losses of the hydrocarbon. The plot described before is exhibited in Figure 5.5.

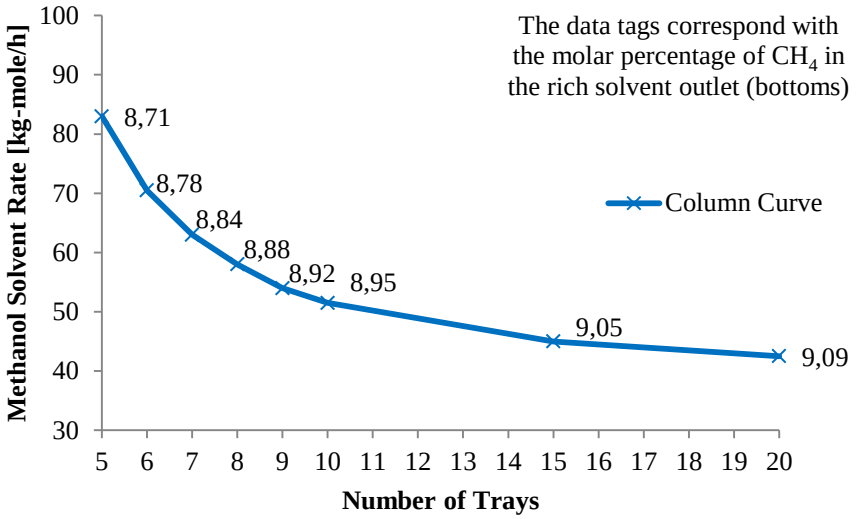

Figure 5.5. Column proficiency profile and CH4 molar percentage for the rich solvent outlet (Solvent Temperature 233,15 K and CO2 heads molar composition 50 ppmv)

Finally, an additional set of plots was constructed in order to observe the ratio between the bottom compositions of CH_4 and CO_2 in function of the number of trays. This latter ratio serves as an efficient operation indicator, being that its value illustrates the relative amount of CO_2 that is absorbed vs. the amount of methane that is lost with the solvent. The higher this value the worst is the operation, as the absorption of methane dominates the processing. Comparative plots for all the temperatures simulated for this ratio vs. number of trays and for the column proficiencies are presented in Figures 5.6 and 5.7, respectively.

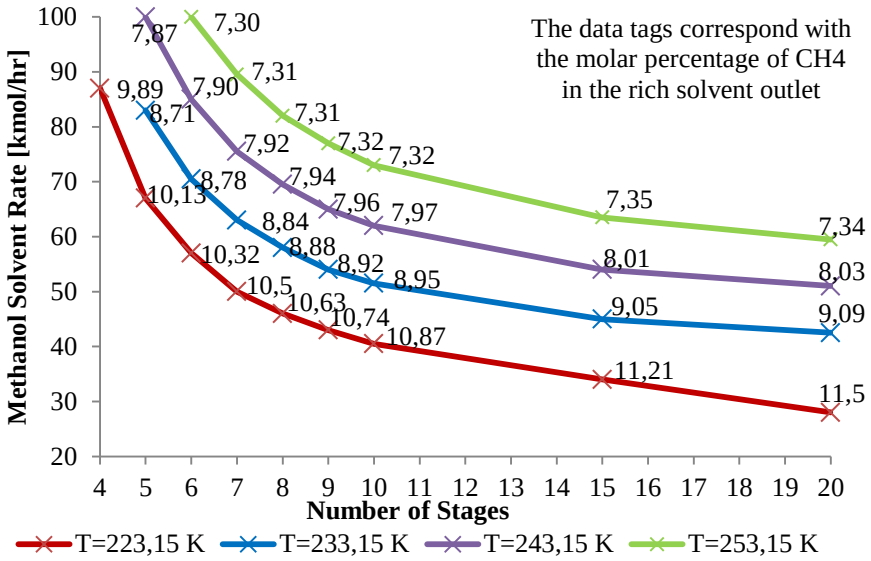

Figure 5.6. Column proficiency profiles and CH_4 molar percentage for the rich solvent outlet (all solvent temperatures simulated at a CO_2 heads molar composition of 50 ppmv)

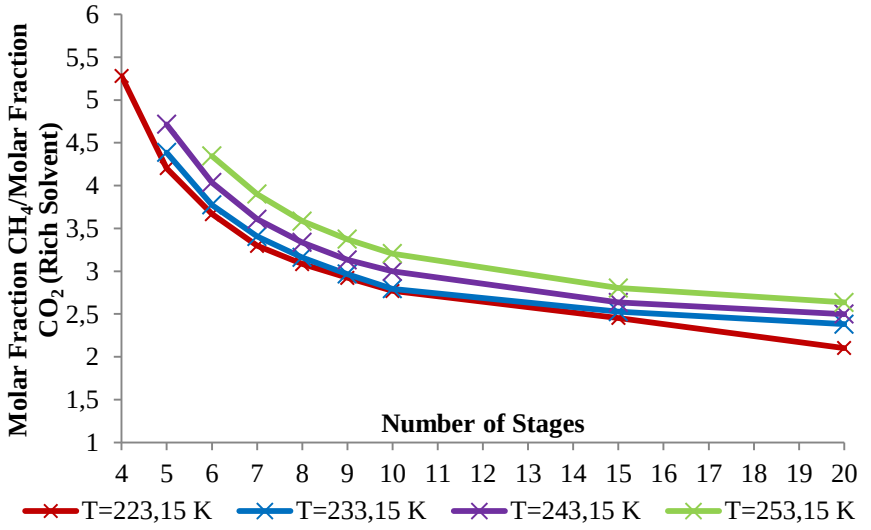

Figure 5.7. Rich Solvent co-absorption ratio between the molar compositions of methanol and carbon dioxide for all the solvent temperatures simulated at a CO_2 heads molar composition of 50 ppmv

5.2.3. Operation point selected

With the information provided in Figures 5.6 and 5.7 it is possible to conclude about the definition of an operation for the absorption unit. First of all, the selected point should complete the following requirements:

- Low value of methane composition in the bottoms. This in order to minimize the losses of the desired gas along with the solvent.
- Low value of co-absorption ratio CH_4/CO_2. This is order to favor the preferred absorption of the contaminant versus the hydrocarbon.
- Intermediate number of stages. As can be seen in Figure 5.3, the higher the number of stages the more complex becomes the modeling of the system; having in some cases non convergence. Moreover, an elevated number of stages imply higher construction costs. Also, a small number of stages is related with higher requirements in solvent input; which translates into higher operations costs and sizing of the equipment [26].
- Low the methanol solvent rate. This is order to reduce pumping costs, pipeline dimensions, etc.

Once understood these restrictions, the different sets of solvent temperature, flow rate and number of stages were analyzed. When analyzing Figure 5.7, the lowest values for the co-absorption ratio are achieved at the lowest temperature simulated: 223,15 K.

Nevertheless, the difference margin between this profile and the one for the next temperature (233,15 K) is not significant for the first stages (up to 10 stages); so that either of these temperatures could be selected. However, the lower the temperature the more

refrigeration will have to be used. Therefore, the selection of 233,15 K was done.

Once the solvent temperature was selected, the number of stages had to be defined. Regarding the restriction of the methane composition in the bottoms, it can be seen from Figure 5.6 that this value stays more or less similar up to 10 stages, starting to increase more significantly for higher number of stages.

As mentioned before, the flow rate increases inversely with the number of stages. Then, in order to handle and adequate flow rate without compromising the amount of methane being co-absorbed; an intermediate value of 10 stages was selected. Finally, the solvent rate was read for this number of stages and before defined solvent temperature. A summarizing list of the selected operation point is presented in Table 5.2.

Table 5.2. Set of variable values selected as the operation point for the absorption unit.

Variable	Value
Solvent temperature	233,15 K
Solvent flow rate	51,5 kg-mole/h
Number of stages	10

5.3. Definition of the Regeneration Stage

Once the CO_2 was effectively absorbed along with the methanol, the regeneration of the solvent had to be studied. As mentioned in previous contents (Chapter 2), the regeneration of the solvent can occur through three main processes: thermal regeneration, inert gas stripping or flash regeneration. The latter was selected as the option to regenerate the solvent in the case of study.

As can be seen in Appendix D, several plant designs for physical solvent processes have regeneration via flashing. The purification technique consists in the selection of different flashing pressures to remove contaminants, such as CO_2 and CH_4 from the rich methanol stream [12].

In this section of the report, as it was done for the absorption stage, a strategy is to be introduced in order to end up with a design for the flashing regeneration units.

5.3.1. Input parameters: variables and assumptions

To begin with the design of this regeneration step, a set of assumptions and parameters were established. The input stream of this section corresponded with the absorption tower outlet bottoms rich solvent. As the first restriction introduced, a maximum CO_2 composition for the lean solvent (after regeneration) stream was set up.

In order to guarantee CO_2 mass transfer from the contaminated gaseous stream into the methanol solvent; the concentration of CO_2 in the liquid phase has to be, at all operating points, less than in the gaseous stream; this to guarantee a concentration gradient between phases. Regarding this mass transfer condition at the top tray, the concentration of the solvent recycle should not be larger than 50 ppmv. This boundary value was selected as the goal CO_2 concentration in the purified solvent stream after the regeneration treatment.

Thus, the pressure difference needed to achieve this concentration was to be determined. In order to find this value, a simple one stage

flashing unit was located after the bottoms outlet of the tower. This flow scheme is illustrated in Figure 5.8.

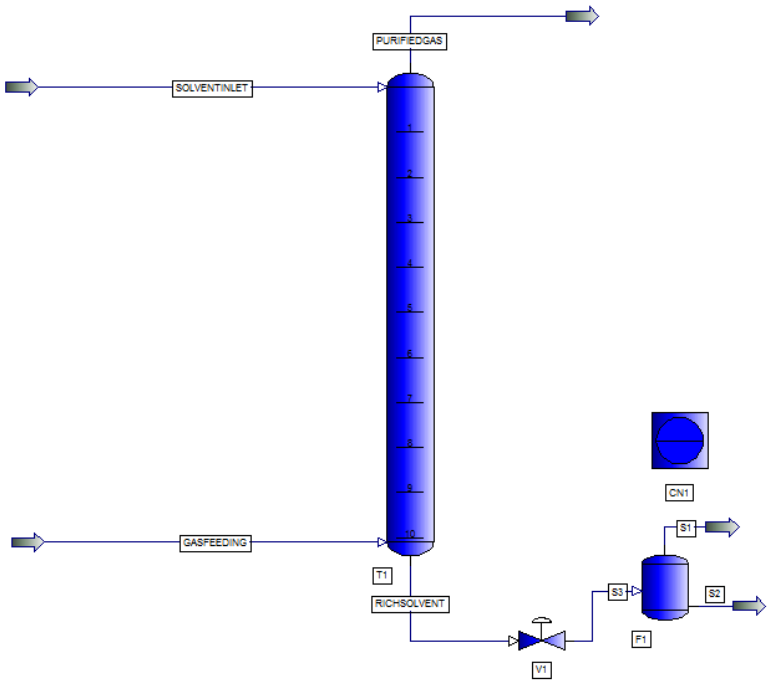

Figure 5.8. Flow scheme simulated to determine the required regeneration pressure gradient.

As seen in the above figure, the rich solvent is throttled through a valve that has variable pressure. The outlet biphasic stream is then flashed adiabatically; resulting as the liquid the lean solvent for recirculation and the gas the CO_2 and CH_4 that remained with the solvent. A controller was set up to vary the valve outlet pressure while maintaining the 50 ppmv constraint in the liquid flash outlet stream.

Summarizing, the value obtained for the outlet pressure in the valve corresponded with a vacuum pressure of 0,051 bar. As stated in the literature [7], vacuum operation is usually present in order to achieve high purity; such as the one established in this case of study. Having and initial pressure of 69,5 bar, the total pressure drop to be distributed within different flashing stages is, therefore, 69,449 bar.

Once this difference was calculated, the pressure distribution came as the second step to be done. To have an idea about the number of stages upon which the distribution could have been done, the literature PFDs included in Appendix D were taken as reference. From this brief analysis, the *Fluor* process (Appendix A-37) one was selected as the simulation pattern (Figure 5.9).

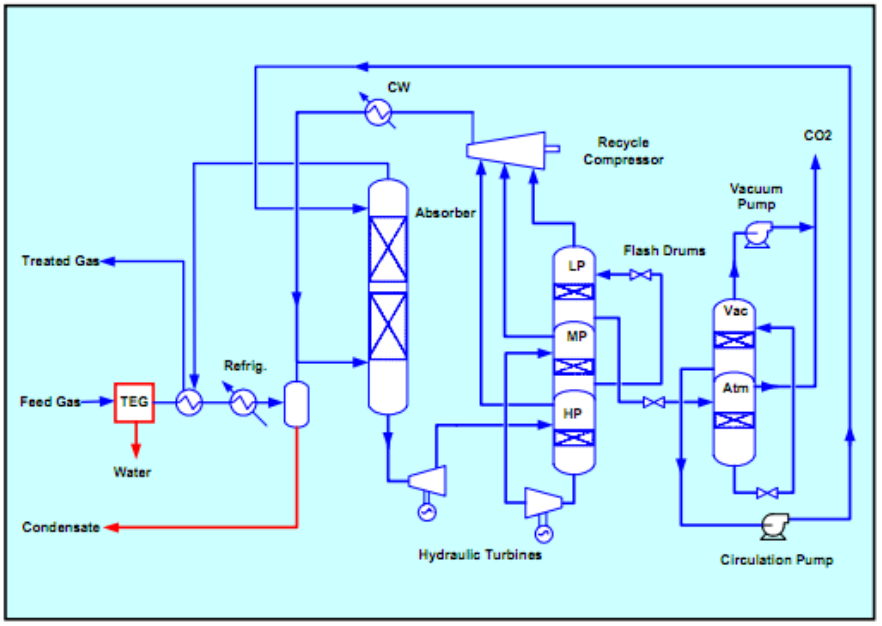

Figure 5.9. Fluor Solvent PFD for low and medium CO_2 inlet concentrations (Appendix A-37)

This figure presents the use of five flash vessels (6 pressure levels) to achieve regeneration. As shown in the figure, there are two groups of vessel tanks: one that generates a gaseous stream to be recycled to the absorber and one that generates a CO_2 waste or injection stream. In the latter group, the nature pressures handled are atmospheric and vacuum.

In the current study, the optimization of intermediate pressures was not addressed. On the other hand, the number of flashing vessels was the main working variable. The pressure levels were selected arbitrarily for each number of flashing vessels; always leaving in place the ambient and vacuum pressures; having then as minimum number of vessels those related to this pressures and the maximum those shown in Figure 5.9 for the *Fluor* process. Also, the temperatures in each flashing stage were not studied and, therefore, the units were assumed adiabatic.

The combinations of the number of flashing units and pressure levels (pressure differences before and after each flashing stage) selected and simulated are presented in Table 5.3.

Table 5.3. Combinations of variables selected for the design of the regeneration stage.

Number of flashing vessels	Pressure levels operated
1	69,5 bar; 0,051 bar
2	69,5 bar; 1,013 bar; 0,051 bar
3	69,5 bar; 35 bar; 1,013 bar; 0,051 bar
4	69,5 bar; 40 bar; 10 bar; 1,013 bar; 0,051 bar
5	69,5 bar; 50 bar; 30 bar; 10 bar; 1,013 bar; 0,051 bar

The procedure followed was to start with a flow scheme for the flashing units similar to that one shown in Figure 5.8 and then, while reducing the number of units, other elements such as expanders, compressors and valves were also removed. The initial five flash regeneration stage flow sheet simulated can be observed in Figure 5.10.

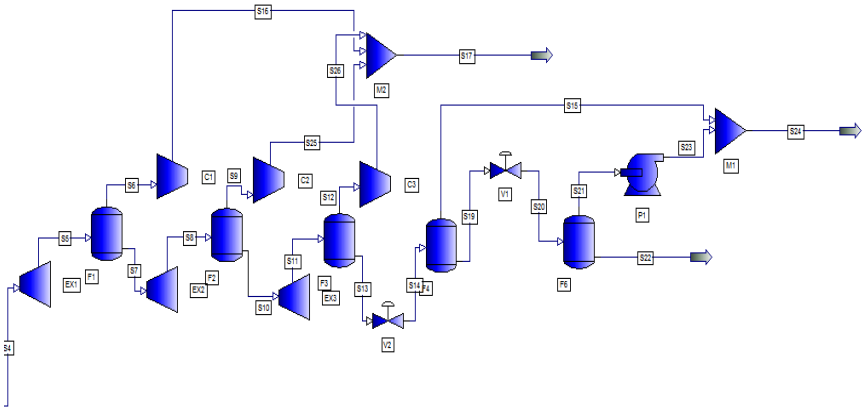

Figure 5.10. Five flashing stages regeneration section of the process simulated

Out of this simulated PFD four streams have to be noted. First, the feeding stream corresponding with the rich methanol stream from the absorption unit. Then, the outlet stream from the three higher pressure levels that corresponds with the gaseous recycle. From the last vacuum flashing stage a liquid regenerated solvent recycle and a gaseous CO_2 rich stream for re-injection.

5.3.2. Results obtained

Once simulated each one of the combinations mentioned in Table 5.3, some results had to be set up as the parameters for selecting an operation configuration. Three parameters were finally disposed for such task.

The first parameter corresponded with the methanol amount that was being recovered in the regeneration stream to be used for future recycling. Then, the same concept was applied to the amount of methane that was being dragged and lost along with this stream.

Finally, the amount of net work output that was being generated with the flow configuration. Evidently, for those configurations without compressors and expanders this variable was avoided. These results are presented in Table 5.4.

Table 5.4. Results for the different unitary configurations for the regeneration stage

Flashing Units Number	Recovered Methanol Percetange	Lost Methane Percetange	Work Generated	Work Consumed	Net Work Output
	%	%	KW	KW	KW
5	99,9784	0,008319	5,4459	4,3777	1,0682
4	99,9786	0,008223	5,8733	3,9746	1,8987
3	99,9821	0,01553	3,0423	1,5055	1,5368
2	99,9810	0,02183	---	---	---
1	99,8326	0,07882	---	---	---

These parameters were plotted for a better comparison in Figures 5.11 to 5.13.

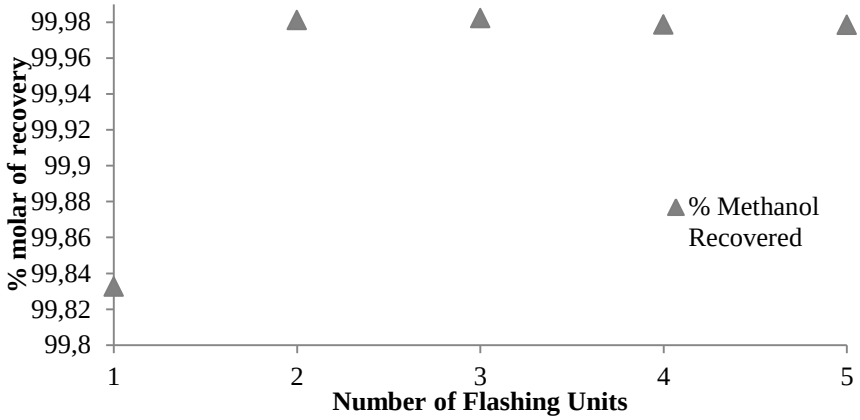

Figure 5.11. Percentage of Methanol Recovery for each Number of flashing Units

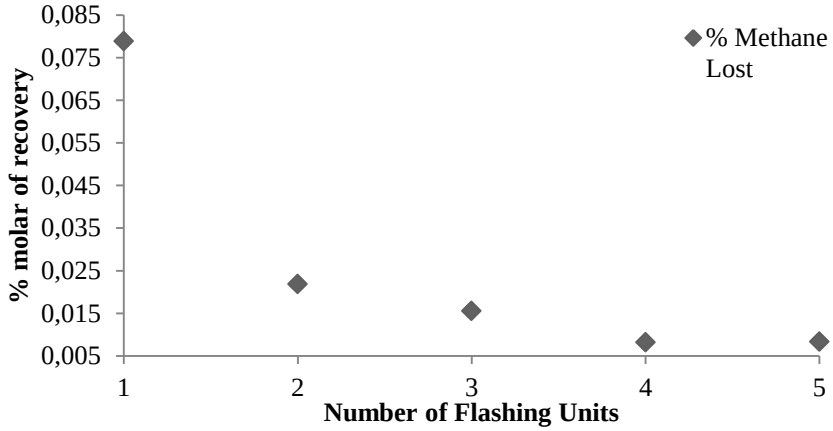

Figure 5.12. Percentage of Methane Lost for each Number of Flashing Units

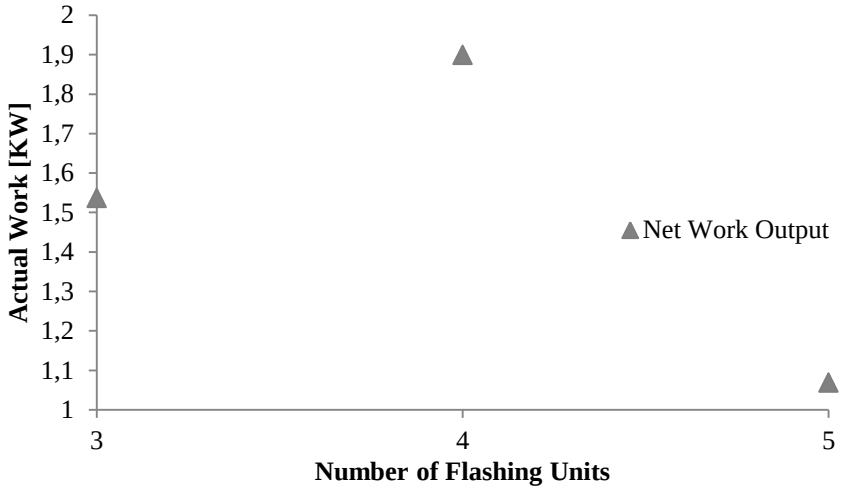

Figure 5.13. Actual Net Work Output for each Number of flashing Units

The methodology behind the calculations of these three parameters is presented ahead. The amount of methanol and methane entering the regeneration unit were calculated. The following expressions were used:

$$\dot{m}_{methanolb} = \dot{m}_{bottoms} \cdot x_{methanolb} \quad (5.1)$$

$$\dot{m}_{methaneb} = \dot{m}_{bottoms} \cdot x_{methaner} \quad (5.2)$$

Where $\dot{m}$ corresponds with the molar flow rates of the component in the bottoms outlet of the absorption unit or with the molar flow rate of the total stream; while *x* corresponds with the molar fraction of the components in this regenerated stream.

Then, similar calculations were done for the regenerated solvent stream:

$$\dot{m}_{methanolr} = \dot{m}_{regenerated} \cdot x_{methanolr} \quad (5.3)$$

$$\dot{m}_{methaner} = \dot{m}_{regenerated} \cdot x_{methaner} \quad (5.4)$$

Where $\dot{m}$ corresponds with the molar flow rates of the component in the outlet stream of the regeneration or with the molar flow rate of the total stream; while *x* corresponds with the molar fraction of the components in this regenerated stream.

Thus, once these two quantities were obtained the percentages were calculated as stated ahead:

$$\%_{methanol} = \dot{m}_{methanolr}/\dot{m}_{methanolb} \quad (5.5)$$

$$\%_{methane} = \dot{m}_{methaner}/\dot{m}_{methaneb} \quad (5.6)$$

Then, to calculate the actual net work output the consumed and produced had to be obtained firstly:

$$W_{consumed} = \sum W_{compressors} + W_{vacuumpump} \quad (5.7)$$

$$W_{produced} = \sum W_{expanders} \quad (5.8)$$

Finally, the net amount was quantity was obtained using the expression stated below:

$$W_{net} = W_{produced} - W_{consumed} \quad (5.9)$$

5.3.3. Operation point selected

Once covered the results for this section of the processing, an operating point had to be selected. From Figures 5.10 to 5.12 and Table 5.4; the configuration selected corresponded with the four flashing units one.

The reasons behind this selection are that with this configuration the smallest amount of CH_4 was being lost, the work output was the highest and, in terms of the amount of methanol recovered, was the second to the best just by a small margin compared to the five flash configuration. Once more, the configuration is summarized in Table 5.5.

Table 5.5. Regeneration configuration selected for operation

Number of flashing vessels	Pressure levels operated
4	69,5 bar; 40 bar; 10 bar; 1,013 bar; 0,051 bar

5.4. Definition of the Heavy Hydrocarbons Pre-treatment

In this pre-treatment stage, two main issues involving the presence of these components inside of the downstream absorption stage are addressed. First of all, the presence of HHC when absorbing with methanol is unwanted in terms of the possible dissolution of this components into the solvent (Chapter 2).

In addition to this problem, due to the low temperatures upon which the tower is operating, the dew point of the mixture could be reached while operation; generating an unwanted hydrocarbon phase inside of the unit.

Due to these reasons, removal of this HHC component is to be done before entering the absorption stage. This removal is achieved through cooling and flashing; operations typically used for this kind of separation (Appendix D).

5.4.1. Identifying the problem: Dew point calculations

To start designing the flashing and cooling units for the system, a dew point calculation ought to be done firstly. This stage of the processing is the first one that addresses multicomponent feeding, so the composition data given for the natural gas stream in Chapter 3 is re-introduced into the analysis. As done in previous sections of this Chapter, the flow rates are scaled down in the same ratio due to computational convergence.

One important assumption made to be able to conduct the simulation of the multiphase stream is that one related to pentane plus component fraction. Lacking information about the molecular weight, normal boiling point and density of this fraction; assuming pure pentane behavior for this component had to be done.

Table 5.6. Composition chart of the natural gas stream to be processed.

Component	Molar Fraction
Methane (C1)	0,830
Ethane (C2)	0,054
Propane (C3)	0,025
Isobutane (i-C4)	0,004
n-Butane (n-C4)	0,007
Pentane plus (C5+)	0,005
Carbon Dioxide (CO_2)	0,050
Nitrogen (N_2)	0,025

Thus, the dew point calculations for the feeding stream were done. To achieve this, a phase envelope diagram was constructed for the stream. Such diagram is presented in Figure 5.14.

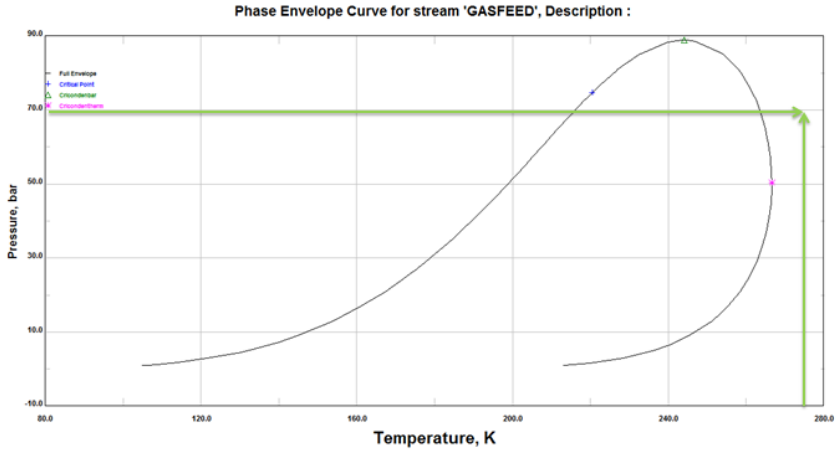

Figure 5.14. Phase envelope for the natural gas feeding with the localization of the feeding point

As can be seen from this figure, the feeding is located afar the dew point line of the envelope. Nevertheless, if the operation point selected in Section 5.2 for the absorber unit is located within the phase diagram, this will be inside the envelope (See Figure 5.15).

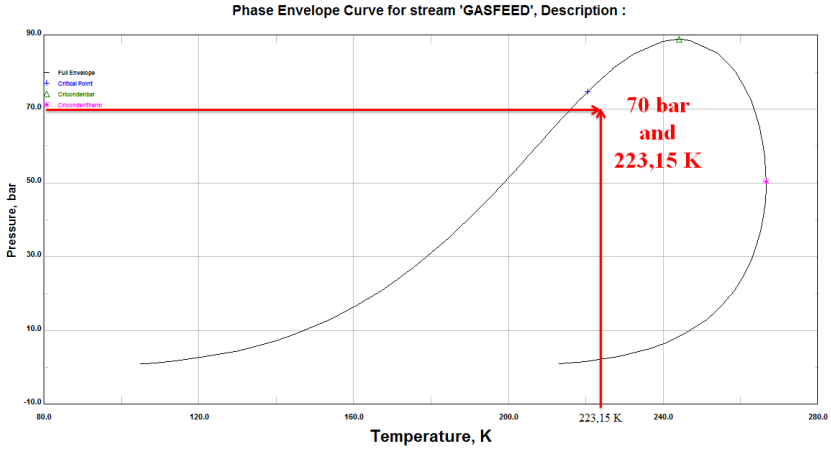

Figure 5.15. Phase envelope for the Feeding Stream with absorber operation point.

5.4.2. Structuration of the HHC processing

In order to avoid the formation of the undesired liquid HHC phase, the absorber should always operate at pressures and temperatures located outside of the phase envelope.

To do so, the dew point should be reduced to lower temperature values; this achieved through the removal of HHC. The feeding stream had to be subject of three processes to reach the appropriate outlet conditions:

- A temperature reduction from the feeding value (283,15K) down to the a final temperature of 218,15 K; 5 degrees below the actual feeding temperature of the absorption process: 223,15 K. This 5 K rise about the new dew point is made in order to guarantee operation outside of the phase envelope [11].
- A subsequent separation of liquid and gaseous streams. This is done with a flash vessel.

The PFD resulting from this unit selection that was simulated is displayed in Figure 5.16:

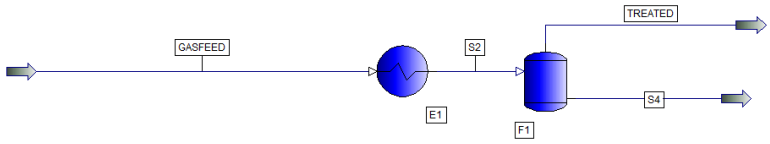

Figure 5.16. PFD simulated for the natural gas pre-treatment

5.4.3. Results obtained

Once the PFD constructed was simulated, a series of results were presented to conclude in terms of the efficiency of the design proposed.

Table 5.7 includes the numerical results of compositions and flow rates after the processing; as well as the percentage of each component that was removed with the HHC pre-treatment.

Table 5.7. Component data before and after the HHC pre-treatment stage

Parameter	Natural Gas Feed	Absorber feed	Percentage removed (%)
Total Flowrate [kg-mole/h]	37,179	28,878	22,326
Methane	0,830	0,863	19,212
Ethane	0,054	0,043	38,260
Propane	0,025	0,015	54,075
Iso-Butane	0,004	0,002	66,966
n-Butane	0,007	0,003	70,718
Pentane	0,005	0,001	83,291
Nitrogen	0,025	0,029	11,098
Carbon Dioxide	0,050	0,045	30,115

As can be observed, the removal of the heavy hydrocarbons is partially achieved; with high percentages for heavier components. Partial removal of CO_2 is also achieved.

On the other hand, a considerable amount of methane is lost during the flashing stage (almost 20%). This can be solved with further flashing stages at different pressure levels, such as what was done for the solvent regeneration. However, the complexity of the design

for this case is evident; since a multicomponent mixture is being simulated. Such an analysis is therefore not addressed.

5.5. Integration of the three stages: final results

After having structured the three main stages involved in the acid gas removal, they ought to be integrated and simulated together in order to establish final conclusions about the design. Ahead, some results concerning calculated and relevant elements for the evaluation of the processing.

Table 5.8. Relative percentages outlet/inlet after all the processing disposed.

Parameter	Percentage Value (%)
HHC (C2+) Removed	91,099
Methane Lost	36,541
CO_2 Removed	97,360
Nitrogen Removed	15,343
Methanol Lost	0,035

Table 5.8 presents percentages regarding the lost or removal of each component of the system simulated. In terms of the Heavy Hydrocarbons, CO_2 and Nitrogen; the percentages refer to removal; as these components are regarded as contaminants along the process. For Methanol and Methane, the percentages are regarded as losses; since these are desired components.

To calculate the percentages, a procedure similar to that stated in Section 5.3 was followed. The plant has two input streams (methanol inlet and gas feed) and four output streams (condensates, purified gas, CO_2 for re-injection and gases removed from the rich solvent).

To calculate all the percentages the molar fractions and flow rates obtained from the simulator were used. All calculations but those for methanol followed this procedure: (an example for methane is selected)

- The amount of methane in the outlet streams, but the purified gas one, is calculated by multiplying the total flow rate of each stream per the local molar composition of methane. Three values are obtained. The purified gas stream is skipped because this is the stream were methane is supposed to be exiting.
- The total amount of methane in the outlets is calculated by adding the three values stated in the last step.
- The amount of methane in the inlet is calculated by multiplying the composition of the substance in the inlet per its total flow rate.
- The percentage is calculating by dividing the amount of methane in the outlets per the amount of methane in the inlet, then multiplying

For methanol, the difference is that instead of using the natural gas feed as inlet the solvent feeding stream is selected.

Once understood the procedure behind the calculations, the percentages can be commented. The high percentage value (91,099 %) for removal of Heavy Hydrocarbons (C2+) indicates that the HHC-pretreatment stage design proposed fulfills the expectations. The same happens for the absorption unit design, achieving a total removal of CO_2 of 97,360 %. In terms of the methanol, the solvent regeneration unit designed is capable of recovering up to 99,965 % of the solvent; an important factor to avoid substantial solvent make-ups (insertion of fresh solvent).

However, the amount of methane lost is substantially high. This is related, mainly, by the lack of several pressure stages in the HHC

Removal process; as mentioned in Section 5.4. This situation indicates the needing of design a methane recovery stage within the processing.

In matters of Nitrogen, the component is also not removed efficiently due to its lightness; reason why it stays with the gas purified stream. Nevertheless, the localization of the nitrogen removal stage is, in most designs, downstream in the processing [11].

Table 5.9. Selected component fractions

Component	Stream	Composition	Requirement
Methane	CO_2 for Injection	31,593 % (molar basis)	2 % (molar basis)
CO_2	Purified Gas	40 ppmv	50 ppmv
Nitrogen	CO_2 for Injection	0,014% (molar basis)	2 % (molar basis)

The information contained in Table 5.9 regards selected compositions of Methane, CO_2 and N_2 that were recalculated once simulating the whole plant and the requirements established in Chapter 3 as quality specifications for further processing.

As can be seen, the purified gas has a concentration of CO_2 lower than the recommendation for LNG further processing; meaning this that the plant design meets the specifications to go into liquefaction.

In terms of the CO_2 possible re-injection for CCS, the amount of nitrogen is significantly below the limits allowed; not being this the case for the methane threshold established. It is possible that, with the inclusion of a methane recovery unit as mentioned before, this specification can be met. Hence, allowing the system to be part of CCS projects.

5.6. Heat Integration with an LNG process

5.6.1. General Definition

First of all, a definition of what heat integration is must be given. Also known as *pinch analysis*, it is a design strategy that calculates and identifies a minimum energy consumption operation (called *energy target*) of the plant through thermodynamic analysis [27].

The optimization is commonly perceived to be achieved with the integration of cold and hot streams within the process inside a heat exchanging unit; but its principles can be extended to power requirements and chemical processing units such as reactors [27].

The strategy followed is to create heat load vs. temperature plots were *composite curves* are illustrated; these being conglomerations of all the hot and the cold streams along the processing, respectively [27].

The relative distance between the two curves indicates the amount of heat that can be exchanged. Those places where the profiles are closer are known as *pinch points* and they represent the values where the heat integration is mostly limited. Hence, once identified, they serve as references to construct heat integration schemes at higher and lower temperatures [27].

The use of pinch analysis implies the reduction of plant costs, given the fact that the dependence of the system of external refrigeration/heating is significantly reduced, e.g.

5.6.2. Feasibility of heat integrating the plant design with LGN processing

Even though a pinch analysis *per se* was not done for the plant design proposed, a simple approach to analyze those places where heat exchanging might be enhanced was conducted.

The first unit that presents the possibility of heat integration is the cooler for reducing the temperature of the gaseous stream from 273,15 K down to 218,15 K.

As part of LNG processing, the liquefaction is achieved through a heat exchanging unit where several refrigeration steps are used to gradually condense all the components presents in the mixture. The heat exchanger follows a complex design where several pure or multicomponent refrigerants serve as sources of heat collection [11].

A first possibility of heat integration might be to include the feeding gas stream into the LNG heat exchanger, this to take advantage of the refrigeration design purposed to cool down the stream without having to recur to more external refrigeration.

The second section of the design that can be subject of pinch analysis is the power outlet generated from the plant processing. As part of the LNG processing, power consuming units such as compressors are used along [11]; this opening the possibility of supplying this energy demand with the available power from the plant design proposed. Table 5.10 includes numerical information of the two energy targets discussed before.

Table 5.10. Energy parameters for the plant design proposed

Parameter	Value
Net work output [KW]	1,919
Heat needed for cooling [KW]	18,917

This information is useful to conduct a heat integration analysis, but as only one heat exchanging unit was included in the design proposed, the realization of a pinch analysis is not worth being done.

5.7. Further Work

Even though the designs proposed for the acid gas removal plant cover mostly the specifications made at the beginning of the project, several points along the simulation work were left as "loose ends" that could, in fact, improve the proximity of the simulated proposed plant and the actual final design. These are included in the following list:

- Extend the design of all the parts of the processing in terms of multicomponent mixtures.
- Perform design of the absorption unit with different configurations, such as packed fillings.
- Complete the HHC removal stage by performing a study of pressure stages and flashing vessels as was done for the solvent regeneration.
- Perform process design for the Nitrogen removal and the Methane recovery.
- Perform calculations for recycling the recovered methanol and other relevant processing streams.
- Conduct a numerical pinch analysis for the design in junction with an LNG processing facility.

6. CONCLUSIONS

The thermodynamic EOS known as SRK-Panagiotopoulos-Reid Modified works as a good alternative to simulate systems related with the acid gas removal; such as those containing methane, methanol, carbon dioxide and hydrogen sulphide. Deviations up to 10% are handled with the simulator model selected.

This thermodynamic tool, in junction with an appropriate simulation program such as Pro II with Provision, can be used for performing calculations to design sour gas treatment processes. In addition, the simulator selected has sufficient information and capability to allow simple plant designs were standard chemical processing units are utilized.

Reduction of CO_2 concentrations in a natural gas stream to values as low as 40 ppmv can be achieved with physical solvent absorption using methanol as the washing stream. Additionally, methanol regeneration from an absorption outlet stream can be accomplished through a successive depressurizing and flashing stages scheme.

On the other hand, heavy-hydrocarbons removal and condensation stages of a sour gas treatment process can be designed from performing dew point calculations for a natural gas stream. These HHC units can be structured by simple processes such as cooling, pressurizing and flashing.

Furthermore, it is possible to achieve processing specifications for a complex multi-stage acid gas removal plant by performing individual step designs and, then, integrating them all.

Finally, there is enough potential within physical methanol absorption to integrate the process to LNG and CCS downstream schemes

7. REFERENCES

[1] International Energy Agency (2009). *World Energy Outlook-2009*. Retrieved May 28-2011, from http://www.iea.org/publications/free_new_Desc.asp?PUBS_ID=2160

[2] Wikipedia (n.d.). *Greenhouse effect.* Retrieved May 28-2011, from http://en.wikipedia.org/wiki/Greenhouse_effect

[3] U.S. Energy Information Administration (2010). Natural Gas. *International Energy Outlook-2010.* Retrieved May 28-2011, from http://www.eia.gov/oiaf/ieo/nat_gas.html

[4] Wikipedia (n.d.). *Reserves-to-production ratio.* Retrieved May 28-2011, from http://en.wikipedia.org/wiki/Reserves-to-production_ratio

[5] Rojey, A.; Jaffret, C.; Carnot-Gandolphe, S.; Durand, B.; Jullian, S.; Valais, M. *Natural Gas: Production, processing and transport.* (2nd ed.). Éditions Technip. Paris, France. Chapter 1 (pp. 20-23) and Chapter 7 (pp. 280-294). 1997.

[6] Kohl, A. Nielsen, R. *Gas Purification* (5th ed.). Gulf Publishing Company. New York, EE.UU. Chapter 14 (pp. 1188-1225). 1997.

[7] Schlumberger (2011). Acid Gas. *Schlumberger Online Glossary*. Retrieved April 22-2011, from http://www.glossary.oilfield.slb.com/search.cfm

[8] Kidnay, A.; Parrish, W. *Fundamentals of Natural Gas Processing.* (1st ed.). Taylor & Francis Group. Boca Raton, U.S.A. Chapter 5 (pp. 91-121). 2006.

[9] *Engineering Data Book* (12th ed.). Gas Processors Supply Association. Tulsa, U.S.A. Sec. 21. 2004b.

[10] Gas Technology Institute (n.d.). *Gas Processing: Acid Gas Removal.* Retrieved April 22-2011, from http://www.gastechnology.org/webroot/app/xn/xd.aspx?it=enweb&xd=1ResearchCap/1_5EandP/1_5_1_AreasOfRsch/Gas_Processing/GP_Acid_Gas_Removal/GP_Acid_Gas_Removal_1_Overview/GP_Acid_Gas_Rmvl_main.xml

[11] Fredheim, A.O. *Gas Processing.* Compendium for the course Industrial Process and Energy Technology (TEP 4185). Energy and Process Engineering Department-NTNU. Tulsa, U.S.A. 2008.

[12] Kohl, A. Nielsen, R. *Gas Purification* (5th ed.). Gulf Publishing Company. New York, U.S.A. Chapter 14 (pp. 1188-1225). 1997.

[13] Burns, D.; Echt, W.I. *Chemical Solvent-based Processes for Acid Gas removal in Gasification Application.* Gasification Technology in Practice: IChemE Conference. Milan, Italy. February 1997.

[14] Wade, L.G. Jr. Amines. *Química Orgánica* (5th ed.). Pearson Education. Madrid, Spain. Chapter 19. 2004.

[15] Wikipedia (n.d.). *Amine Gas Treating.* Retrieved April 30-2011, from http://en.wikipedia.org/wiki/Amine_gas_treating

[16] Lurgi A.D. (n.d.) *The Rectisol Process.* Retrieved May 5-2011, from http://www.lurgi.com/website/fileadmin/user_upload/1_PDF/1_Broshures_Flyer/englisch/0308e_Rectisol.pdf

[17] Offshore Technology (2011). *Snøhvit Gas Field, Barents Sea, Norway.* Retrieved May 30-2011, from http://www.offshore-technology.com/projects/snohvit/

[18] Statoil (2007). *Snøhvit.* Retrieved May 30-2011, from http://www.statoil.com/en/OurOperations/ExplorationProd/ncs/snoehvit/Pages/default.aspx

[19] *Chemical Design and Process Simulation Software.* Retrieved May 15-2011, from http://www.business.com/directory/chemicals/software/design_and_process_simulation/

[20] Invensys (2011). *Pro/II Comprehensive Process Simualtion*. Retrieved May 15-2011, from http://iom.invensys.com/EN/Pages/SimSci-Esscor_ProcessEngSuite_PROII.aspx

[21] Invensys (2009). *Pro/II 8.3 User's Manual.* Computational Help included in the Program.

[22] Craig, D. *Disadvantages of Simulation.* Computer Science Department. Memorial University. Newfoundland, Canada. 1996. Retrieved May 15-2011, from http://web.cs.mun.ca/~donald/msc/node7.html

[23] Twu, C.H.; Coon, J.E.; Kusch, M.; Harvey, A.H. *Selection of Equations of State Models for Process Simulator*. Simsci-Esscor. California, U.S.A. 1994. Retrieved May 20-2011, from http://www.sim4me.com.cn/userfiles/file/0908101244040506.pdf

[24] Green, D.; Perry, R. *Perry's Chemical Engineers' Manual* (8th ed.). McGraw Hill. New York, U.S.A. Chapter 2. 2007.

[25] Gutiérrez, E. *Química* (1st ed.). Reverté. Barcelona, Spain. Chapter 6 (pp. 182). 1985.

[26] Hines, A.L. Maddox, R.N. *Transferencia de Masa: fundamentos y aplicaciones* (1st. ed). Prentice Hall. Mexico City, Mexico. 1987.

[27] Kemp, I.C. *Pinch Analysis and Process Integration* (2nd ed.). Elsevier. Oxford, U.K. Chapter 1 (pp. 1-11). 2007.

[28] International Union of Pure and Applied Chemistry (IUPAC). *Carbon Dioxide in non-Aqueous Solvents at Pressures less than 200 KPA* (1st ed.).Solubility Data Series. Frankfurt/Main, Germany. Vol. 50 (pp. 140). 1992.

[29] Deutsche Gesellschaft für Chemisches Apparatewesen (DECHEMA). *Vapor-Liquid Equilibria for Mixtures of Low Boiling Substances* (1st ed.). Chemistry Data Series. Oxford, U.K. Vol. VI (pp. 621-624). 1982.

[30] Weber, W.; Zeck, S.; Knapp, H. *Gas Solubilities in Liquid Solvents at High Pressures: Apparatus and Results for Binary and Ternary Systems of N_2, CO_2 and CH_3OH.* Institute of Thermodynamics and Plant Design. Technical University of Berlin. Berlin, Germany. 1985.

[31] Chang, T.; Rousseau, R. *Solubilites of Carbon Dioxide in Methanol and Methanol-Water at High Pressures: Experimental Data and Modeling.* Department of Chemical Engineering. North Carolina State University. Raleigh, U.S. 1985.

[32] Chang, C.; Chany-Yih, D.; Ching-Ming, K.; Kou-Lung, C. *Densities and P-x-y diagrams for carbon dioxide dissolution in methanol, ethanol and acetone mixtures.* Department of Chemical Engineering. National Chun-Hsing University. Taichung, Taiwan. 1996.

[33] Oghaki, K.; Katayama, T. *Isothermal Vapor-Liquid Equilibrium Data for Binary Systems Containing Carbon Dioxide at High Pressures: Methanol-Carbon Dioxide, n-Hexane-Carbon Dioxide, and Benzene-Carbon Dioxide Systems.* Department of Chemical Engineering. Osaka University. Toyonaka, Japan. 1976.

[34] Leu, C. J.; Robinson, D.B.; *The equilibrium phase properties of the metanol-hydrogen sulfide binary system.* Fluid Phase Equilibrium. Vol. 72 (pp. 163-172). 1992.

[35] Hong, J.H.; Malone, P.V.; Jett, M.D.; Kobayashi, R. *The Measurement and Interpretation of the Fluid Phase Equilibria of a Normal Fluid in a Hydrogen Bonding Solvent: The Methane-Methanol System.*Department of Chemical Engineering, Rice University. Houston, U.S. 1987

[36] Mak, J.; Wierenga, D.; Nielsen, D.; Graham, O. *New Physicial Solvent Treating Configurations for Offshore High Pressure CO_2 Removal.* Fluor Enterprises, Inc. California, U.S. 2003.

APPENDIXES

APPENDIX A: Thermodynamic Data for the Methanol-CO_2 System

Appendix A-1. Methanol-CO_2 data at T=194,5 K [28]

Reference	Pressure	CO_2 liquid mole fraction		Percentage Error
	[bar]	Research	Simulated	%
IUPAC (1992)	0,133	0,036	0,014	60,894
	0,400	0,107	0,046	57,130
	0,667	0,179	0,083	53,501
	1,013	0,250	0,143	42,800

Appendix A-2. Methanol-CO2 data at T=202,6 K [28]

Reference	Pressure	CO_2 liquid mole fraction		Percentage Error
	[bar]	Research	Simulated	%
IUPAC (1992)	0,133	0,022	0,010	54,955
	0,400	0,067	0,031	53,453
	0,667	0,114	0,054	52,548
	1,013	0,171	0,088	48,387

Appendix A-3. Methanol-CO2 data at T=212,7 K [28]

Reference	Pressure	CO_2 liquid mole fraction		Percentage Error
	[bar]	Research	Simulated	%
IUPAC (1992)	0,133	0,013	0,007	46,154
	0,400	0,039	0,021	45,876
	0,667	0,065	0,036	44,530
	1,013	0,098	0,056	42,564

Appendix A-4. Methanol-CO2 data at T=213,15 K [29]

Reference	Pressure	CO_2 liquid mole fraction		Percentage Error
	[bar]	Research	Simulated	%
DECHEMA (1982)	1,013	0,089	0,055	38,272
	2,026	0,186	0,125	32,796
	3,040	0,312	0,228	26,923
	4,255	0,580	0,544	6,207

Appendix A-5. Methanol-CO2 data at T=227,9 K [28]

Reference	Pressure	CO_2 liquid mole fraction		Percentage Error
	[bar]	Research	Simulated	%
IUPAC (1992)	0,133	0,007	0,004	39,394
	0,400	0,020	0,012	38,463
	0,667	0,034	0,021	37,313
	1,013	0,051	0,033	34,653

Appendix A-6. Methanol-CO_2 data at T=228,15 K [29]

Reference	Pressure	CO_2 liquid mole fraction		Percentage Error
	[bar]	Research	Simulated	%
DECHEMA (1982)	1,013	0,048	0,032	33,333
	2,026	0,095	0,068	28,042
	3,040	0,144	0,109	24,306
	4,053	0,200	0,158	21,000
	5,066	0,264	0,218	17,424
	7,093	0,450	0,492	-9,333
	8,309	1,000	0,964	3,600

Appendix A-7. Methanol-CO_2 data at T=233,15 K [30]

Reference	Pressure	CO_2 liquid mole fraction		Percentage Error
	[bar]	Research	Simulated	%
Weber et al, (1984)	2,960	0,113	0,088	10,619
	4,272	0,171	0,138	19,440
	5,427	0,234	0,190	18,803
	6,167	0,280	0,231	17,441
	8,239	0,469	0,437	6,743
	8,781	0,539	0,563	-4,530

Appendix A-8. Methanol-CO_2 data at T=237,15 K [29]

Reference	Pressure	CO_2 liquid mole fraction		Percentage Error
	[bar]	Research	Simulated	%
DECHEMA (1982)	1,013	0,035	0,025	28,571
	2,026	0,070	0,051	27,143
	3,040	0,100	0,080	20,000
	4,053	0,140	0,111	20,714
	5,066	0,178	0,147	17,416
	7,093	0,274	0,237	13,504
	8,309	0,338	0,315	6,805
	10,132	0,467	---	---
	11,652	1,000	---	---

Appendix A-9. Methanol-CO_2 data at T=240,7 K [28]

Reference	Pressure	CO_2 liquid mole fraction		Percentage Error
	[bar]	Research	Simulated	%
IUPAC (1992)	0,133	0,004	0,003	23,077
	0,400	0,012	0,009	23,077

Appendix A-9 Continued

0,667	0,020	0,014	29,648
1,013	0,031	0,022	28,105

Appendix A-10. Methanol-CO_2 data at T=243,15 K [31]

Reference	Pressure	CO_2 liquid mole fraction		Percentage Error
	[bar]	Research	Simulated	%
Chang et Rousseau (1985)	2,003	0,059	0,042	28,571
	4,687	0,150	0,108	28,000
	7,015	0,231	0,180	21,977
	9,778	0,351	0,302	13,837
	12,234	0,534	0,680	-27,365
	13,103	0,715	0,912	-27,481

Appendix A-11. Methanol-CO_2 data at T=247,15 K [29]

Reference	Pressure	CO_2 liquid mole fraction		Percentage Error
	[bar]	Research	Simulated	%
DECHEMA (1982)	1,013	0,025	0,019	22,764
	2,026	0,050	0,038	23,695
	3,040	0,073	0,059	19,178
	4,053	0,100	0,081	18,593
	5,066	0,126	0,105	16,667
	7,093	0,182	0,158	13,187
	8,309	0,216	0,195	9,722
	10,132	0,278	0,263	5,396
	11,652	0,330	0,34	-3,030
	15,199	0,622	---	---

Appendix A-12. Methanol-CO_2 data at T=248 K [28]

Reference	Pressure	CO_2 liquid mole fraction		Percentage Error
	[bar]	Research	Simulated	%
IUPAC (1992)	0,133	0,003	0,002	36,909
	0,400	0,010	0,007	26,548
	0,667	0,016	0,012	24,481
	1,013	0,024	0,018	25,589

Appendix A-13. Methanol-CO_2 literature at T=253,15 K [30]

Reference	Pressure	CO_2 liquid mole fraction		Percentage Error
	[bar]	Research	Simulated	%
Weber et al, (1984)	5,476	0,115	0,096	16,303
	7,203	0,159	0,133	16,141
	9,472	0,226	0,188	16,814
	10,952	0,279	0,230	17,681
	13,813	0,404	0,341	15,531
	14,997	0,490	0,413	15,680

Appendix A-14. Methanol-CO_2 data at T=258,15 K [31]

Reference	Pressure	CO_2 liquid mole fraction		Percentage Error
	[bar]	Research	Simulated	%
Chang et Rousseau (1985)	2,161	0,040	0,031	22,111
	5,427	0,106	0,084	20,455
	10,182	0,207	0,176	14,976
	15,638	0,348	0,335	3,597
	18,875	0,485	0,578	-19,298
	20,996	0,718	0,917	-27,734

Appendix A-15. Methanol-CO_2 data at T=273,15 K [28, 30, 31]

Reference	Pressure	CO_2 liquid mole fraction		Percentage Error
	[bar]	Research	Simulated	%
Chang et Rousseau, (1985)	1,885	0,023	0,020	12,281
	5,081	0,064	0,055	14,463
	10,597	0,137	0,124	9,357
	20,345	0,283	0,284	-0,211
	27,764	0,445	0,551	-23,792
	31,494	0,646	0,906	-40,204
Weber et al, (1984)	4,420	0,058	0,048	16,955
	8,485	0,099	0,096	3,421
	12,530	0,153	0,150	1,639
	15,688	0,197	0,198	-0,304
	21,213	0,282	0,303	-7,409
	23,285	0,329	0,355	-7,936
	25,357	0,374	0,422	-12,744
	30,882	0,559	0,875	-56,474
	32,559	0,763	0,945	-23,805
IUPAC (1992)	0,133	0,002	0,001	36,306
	0,400	0,005	0,004	14,894
	0,667	0,008	0,007	10,600
	1,013	0,012	0,010	15,966

Appendix A-16. Methanol-CO_2 data at T=291,15 K [32]

Reference	Pressure	CO_2 liquid mole fraction		Percentage Error
	[bar]	Research	Simulated	%
Chang et al, (1997)	5,6	0,060	0,044	26,050
	6,7	0,071	0,053	25,666
	8,9	0,095	0,071	25,263

Appendix 16 Continued

11,8	0,127	0,097	23,502
17,6	0,200	0,151	24,500
23,6	0,291	0,214	26,435
28,1	0,3579	0,268	25,119
31,0	0,4025	0,307	23,723
34,6	0,4504	0,364	19,183
38,4	0,5807	0,441	24,057
43,3	0,7575	0,714	5,473
49,3	0,8835	0,921	-4,244

Appendix A-17. Methanol-CO_2 data at T=298,15 K [30, 31, 32, 33]

Reference	Pressure	CO_2 liquid mole fraction		Percentage Error
	[bar]	Research	Simulated	%
Oghaki and Katayama (1976)	7,641	0,060	0,055	7,718
	18,450	0,155	0,143	7,623
	29,661	0,260	0,251	3,499
	38,739	0,350	0,364	-4,149
	47,723	0,489	0,554	-13,385
	53,949	0,645	0,861	-33,468
	56,397	0,769	0,923	-20,104
	57,613	0,900	0,944	-4,866
Chang et Rousseau (1985)	2,536	0,018	0,017	5,556
	5,427	0,039	0,038	2,813
	10,153	0,073	0,074	-0,955
	17,148	0,130	0,131	-0,769
	29,392	0,230	0,246	-7,143
	39,318	0,333	0,369	-10,678
	47,004	0,435	0,523	-20,119
	53,102	0,568	0,814	-43,234

Appendix A-17 Continued

Chang et al, (1997)	9,2	0,071	0,066	6,516
	12,7	0,100	0,093	6,533
	16,2	0,130	0,121	6,564
	19,6	0,160	0,149	6,642
	22,8	0,189	0,178	5,570
	26,0	0,218	0,208	4,500
	29,6	0,250	0,244	2,517
	33,3	0,284	0,284	-0,141
	36,5	0,313	0,323	-3,129
	40,0	0,349	0,372	-6,560
	43,4	0,392	0,428	-9,323
	46,9	0,444	0,503	-13,416
	50,3	0,509	0,617	-21,194
	53,8	0,591	0,813	-37,680
	55,0	0,698	0,860	-23,227
	56,0	0,780	0,890	-14,103
	57,1	0,884	0,915	-3,507
Weber et al, (1984)	7,696	0,062	0,054	12,338
	9,837	0,079	0,070	11,504
	14,415	0,115	0,106	7,585
	17,523	0,143	0,132	7,886
	20,739	0,166	0,159	4,159
	21,765	0,177	0,168	4,870
	29,313	0,255	0,241	5,564
	34,079	0,305	0,293	3,997
	37,394	0,344	0,335	2,729
	46,353	0,480	0,489	-1,875
	50,151	0,557	0,610	-9,456

Appendix A-18. Methanol-CO_2 data at T=303,15 K [32]

Reference	Pressure	CO_2 liquid mole fraction		Percentage Error
	[bar]	Research	Simulated	%
Chang et al, (1997)	8,9	0,069	0,058	15,820
	13,1	0,092	0,088	4,762
	16,5	0,120	0,113	6,146
	20,1	0,151	0,141	6,561
	24,3	0,181	0,175	3,528
	29,1	0,215	0,216	-0,279
	34,2	0,2571	0,264	-2,684
	38,9	0,2972	0,313	-5,316
	42,5	0,3245	0,356	-9,707
	45,6	0,3507	0,397	-13,202
	49,4	0,4005	0,458	-14,357
	53,1	0,4777	0,537	-12,414
	55,8	0,546	0,623	-14,207
	59,3	0,629	0,797	-26,689
	61,7	0,708	0,88	-24,241
	63,2	0,883	0,913	-3,362

Appendix A-19. Methanol-CO_2 data at T=308,15 K [32]

Reference	Pressure	CO_2 liquid mole fraction		Percentage Error
	[bar]	Research	Simulated	%
Chang et al, (1997)	13,2	0,087	0,082	5,639
	17,1	0,110	0,109	1,089
	21,1	0,143	0,137	4,196
	25,8	0,176	0,172	2,106
	31,3	0,210	0,215	-2,430
	36,5	0,243	0,259	-6,584

Appendix A-19 Continued

40,0	0,2668	0,291	-9,070
43,9	0,2971	0,330	-11,074
48,7	0,3391	0,384	-13,241
51,6	0,3668	0,422	-15,049
56,8	0,4337	0,506	-16,671
60,1	0,5025	0,581	-15,622
63,1	0,582	0,685	-17,718
66,6	0,647	0,838	-29,441
68,9	0,808	0,897	-11,015
70,1	0,884	0,919	-3,995

Appendix A-20. Methanol-CO_2 data at T=313,15 K [32, 33]

Reference	Pressure	CO_2 liquid mole fraction		Percentage Error
	[bar]	Research	Simulated	%
Oghaki and Katayama (1976)	5,587	0,029	0,030	-5,263
	17,131	0,102	0,101	1,271
	29,081	0,164	0,181	-10,299
	39,557	0,234	0,261	-11,586
	55,224	0,366	0,412	-12,722
	60,706	0,420	0,485	-15,449
	68,652	0,543	0,629	-15,859
	74,551	0,689	0,873	-26,669
	77,992	0,897	0,934	-4,125
Chang et al, (1997)	13,2	0,068	0,076	-11,437
	16,7	0,091	0,098	-7,574
	20,3	0,116	0,122	-5,263
	24,7	0,137	0,151	-10,058
	31,3	0,177	0,197	-11,111
	36,1	0,201	0,233	-16,152

Appendix A-20 Continued

39,6	0,238	0,261	-9,618
45,6	0,273	0,313	-14,526
55,0	0,346	0,409	-18,072
59,1	0,384	0,461	-20,115
62,0	0,413	0,505	-22,335
66,0	0,466	0,584	-25,376
69,0	0,514	0,602	-17,166
70,6	0,547	0,735	-34,443
73,9	0,591	0,857	-45,082
76,9	0,682	0,919	-34,830
80,3	0,878	---	---

APPENDIX B: Thermodynamic Data for the Methanol-H_2S System

Appendix B-21. Methanol-H_2S data at T=298,15 K [34]

Reference	Pressure	H_2S liquid mole fraction		Percentage Error
	[bar]	Researched	Simulated	%
Leu et al, (1991)	0,173	0,000	0,000	0
	0,865	0,017	0,018	-9,091
	2,875	0,068	0,072	-5,882
	4,861	0,135	0,131	3,250
	9,032	0,289	0,285	1,452
	12,330	0,424	0,458	-8,095
	15,660	0,605	0,714	-18,114
	17,670	0,790	0,866	-9,606
	18,840	0,917	0,935	-1,952
	19,840	0,989	0,983	0,587
	20,220	1,000	1	0

Appendix B-22. Methanol-H_2S data at T=348,15 K [34]

Reference	Pressure	H_2S liquid mole fraction		Percentage Error
	[bar]	Researched	Simulated	%
Leu et al, (1991)	1,51	0,000	0,000	0
	1,76	0,002	0,003	-31,579
	4,23	0,029	0,034	-15,646
	4,36	0,033	0,036	-9,422
	6,99	0,066	0,07	-5,581
	12,60	0,126	0,147	-16,574
	12,90	0,136	0,151	-11,111
	22,20	0,265	0,297	-12,033

Appendix B-22 Continued

24,40	0,313	0,336	-7,348
36,30	0,542	0,584	-7,670
41,10	0,629	0,698	-10,899
44,7	0,7389	0,781	-5,698
51,2	0,9053	0,906	-0,077
54,7	0,9712	0,958	1,359
56,6	0,9938	0,982	1,187
58	1	1	0

Appendix B-23. Methanol-H2S data at T=388,15 K [24]

Reference	**Pressure**	**H_2S liquid mole fraction**		**Percentage Error**
	[bar]	**Researched**	**Simulated**	**%**
Leu et al, (1991)	7,38	0,000	0,000	0
	9,24	0,016	0,019	-17,284
	15,20	0,063	0,084	-33,122
	21,40	0,110	0,139	-26,134
	30,60	0,192	0,226	-17,586
	47,40	0,344	0,4	-16,381
	59,00	0,435	0,532	-22,187
	71,30	0,559	0,68	-21,624
	82,90	0,683	0,81	-18,594
	90,50	0,762	0,883	-15,864
	92,90	0,784	0,903	-15,193
	97,8	0,8383	---	---
	99,7	0,8606	---	---
	101	0,882	---	---

Appendix B-24. Methanol-H2S data at T=448,15 K [24]

Reference	Pressure	H_2S liquid mole fraction		Percentage Error
	[bar]	Researched	Simulated	%
Leu et al, (1991)	24,2	0,000	0,000	0
	24,5	0,002	---	---
	26,1	0,012	0,010	13,043
	31,4	0,036	0,042	-17,318
	33,4	0,053	0,053	0,188
	45,4	0,136	0,126	7,489
	58,6	0,211	0,208	1,375
	85,0	0,364	0,379	-4,207
	97,4	0,446	0,462	-3,680
	107,0	0,516	0,538	-4,223
	108,0	0,530	0,546	-3,038
	109	0,5442	0,555	-1,985
	111	0,5737	0,572	0,296
	112	0,6048	0,582	3,770

APPENDIX C: Thermodynamic Data for the Methanol-Methane System

Appendix C-25. Methanol-CH_4 data at T=200 K [35]

Reference	Pressure	CH_4 liquid mole fraction		Percentage Error
	[bar]	Researched	Simulated	%
Hong et al, (1991)	13,789	0,029	0,044	-53,150
	34,473	0,071	0,095	-34,371
	51,711	0,099	0,122	-23,096
	68,947	0,112	0,134	-19,857
	103,421	0,121	0,145	-19,538
	137,895	0,129	0,154	-19,195
	206,842	0,143	0,168	-17,647
	275,789	0,154	0,179	-16,536
	344,737	0,164	0,189	-15,526
	413,685	0,176	0,198	-12,821

Appendix C-26. Methanol-CH_4 data at T=220 K [35]

Reference	Pressure	CH_4 liquid mole fraction		Percentage Error
	[bar]	Researched	Simulated	%
Hong et al, (1991)	6,847	0,010	0,014	-34,486
	13,789	0,020	0,028	-41,058
	34,473	0,052	0,063	-20,413
	51,711	0,077	0,086	-12,374
	68,947	0,095	0,102	-7,120
	103,421	0,119	0,12	-0,925
	137,895	0,131	0,132	-0,610
	206,842	0,151	0,148	1,987
	275,789	0,169	0,16	5,045

Appendix C-26 Continued

344,737	0,180	0,171	5,158
413,685	0,193	0,18	6,784

Appendix C-27. Methanol-CH_4 data at T=250 K [35]

Reference	Pressure	CH_4 liquid mole fraction		Percentage Error
	[bar]	Researched	Simulated	%
Hong et al, (1991)	13,789	0,016	0,019	-21,873
	34,473	0,038	0,043	-14,240
	51,711	0,056	0,061	-9,260
	68,947	0,073	0,075	-3,206
	103,421	0,101	0,098	2,681
	137,895	0,122	0,114	6,862
	172,368	0,138	0,126	8,695
	206,842	0,152	0,135	11,184
	275,789	0,176	0,151	14,058
	344,737	0,196	0,164	16,454
	413,685	0,215	0,175	18,490

Appendix C-28. Methanol-CH_4 data at T=273,15 K [35]

Reference	Pressure	CH_4 liquid mole fraction		Percentage Error
	[bar]	Researched	Simulated	%
Hong et al, (1991)	13,789	0,013	0,015	-13,809
	34,473	0,032	0,036	-12,360
	51,711	0,047	0,052	-10,216
	68,947	0,062	0,066	-6,796
	103,421	0,089	0,089	0,146
	137,895	0,113	0,107	5,058
	172,368	0,133	0,121	8,748

		Appendix C-28 Continued		
	206,842	0,149	0,133	10,558
	241,316	0,165	0,143	13,123
	275,789	0,179	0,152	15,273
	344,737	0,204	0,168	17,687
	413,685	0,228	0,180	21,191

Appendix C-29. Methanol-CH_4 data at T=290 K [35]

Reference	**Pressure**	**CH_4 liquid mole fraction**		**Percentage Error**
	[bar]	**Researched**	**Simulated**	**%**
Hong et al, (1991)	13,789	0,012	0,014	-19,658
	27,579	0,023	0,027	-15,385
	41,368	0,035	0,040	-15,473
	68,947	0,057	0,062	-9,502
	86,184	0,071	0,075	-6,353
	103,421	0,084	0,086	-2,970
	137,895	0,106	0,105	1,130
	172,368	0,126	0,121	4,272
	206,842	0,146	0,134	8,345
	275,789	0,181	0,156	13,717
	344,737	0,210	0,174	17,222
	413,685	0,239	0,188	21,273

Appendix C-30. Methanol-CH_4 data at T=310 K [35]

Reference	**Pressure**	**CH_4 liquid mole fraction**		**Percentage Error**
	[bar]	**Researched**	**Simulated**	**%**
Hong et al, (1991)	13,789	0,011	0,013	-22,873
	27,579	0,021	0,026	-22,990
	41,368	0,032	0,038	-20,597

Appendix C-30 Continued

55,157	0,042	0,049	-16,694
68,947	0,052	0,06	-14,569
82,737	0,063	0,07	-11,447
96,526	0,073	0,08	-10,026
117,211	0,087	0,093	-6,468
137,895	0,102	0,105	-3,143
172,368	0,123	0,123	-0,326
206,842	0,142	0,138	3,021
241,316	0,162	0,152	6,231
275,789	0,181	0,164	9,141
310,264	0,198	0,174	12,121
344,737	0,215	0,184	14,219
413,685	0,244	0,201	17,657

Appendix C-31. Methanol-CH_4 data at T=330 K [35]

Reference	Pressure	CH_4 liquid mole fraction		Percentage Error
	[bar]	Researched	Simulated	%
Hong et al, (1991)	13,789	0,009	0,012	-26,823
	34,473	0,025	0,031	-25,608
	51,711	0,037	0,046	-23,424
	68,947	0,050	0,060	-20,385
	103,421	0,073	0,085	-15,741
	137,895	0,097	0,108	-11,582
	172,368	0,119	0,127	-6,812
	206,842	0,141	0,145	-3,056
	275,789	0,182	0,174	4,185
	344,737	0,222	0,198	10,730
	413,685	0,258	0,218	15,340

APPENDIX D: Additional Information of Physical Solvent Processes

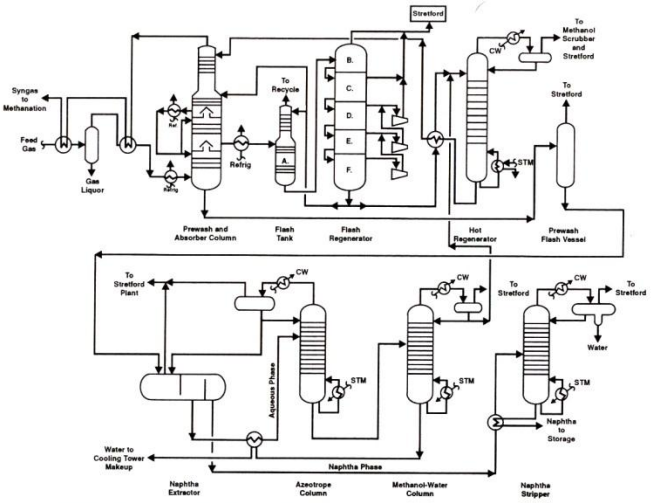

Figure 14-17. Simplified process flow diagram of Rectisol process system at the SNG-from-coal plant in North Dakota. (*Miller and Lang, 1985*)

Appendix D-32. Standard Rectisol simplified plant diagram for a Syngas process. North Dakota, U,S, [12]

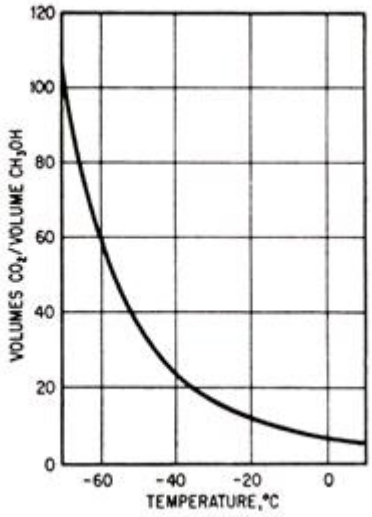

Appendix D-33. Solubility of CO_2 in Methanol at a Partial CO_2 pressure of 1 atm [12]

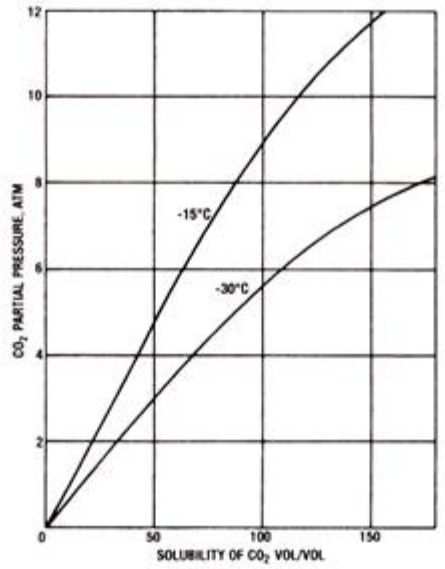

Appendix D-34. Effect of Partial Pressure on the Solubility of CO_2 in Methanol [12]

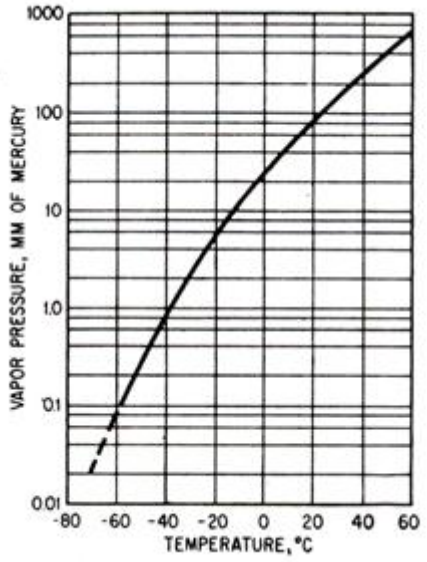

Appendix D-35. Vapor Pressure of Methanol [12]

Table 14-18
Equilibrium Solubilities of H_2S and CO_2 in Methanol

Temperature, °C	Solubility, vol/vol		Selectivity
	H_2S	CO_2	H_2S/CO_2
−10	41	8	5.1
−30	92	15	6.1

Source: Data of Hochgesand (1970)

Appendix D-36. Equilibrium Solubilities of H_2S and CO_2 with Methanol as a solvent [12]

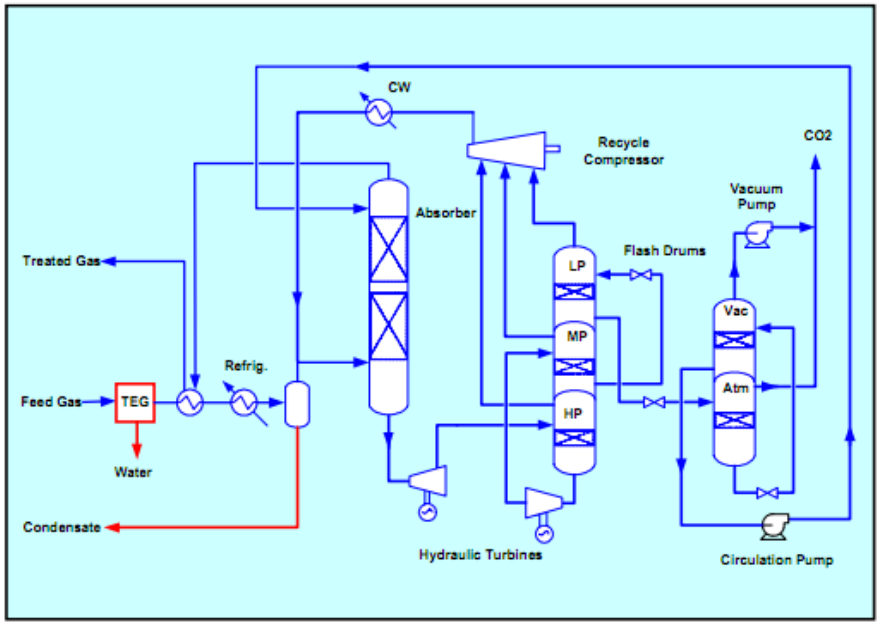

Appendix D-37. Fluor Solvent PFD for low and medium CO_2 inlet concentrations [36]